Technical report on operating accelerators 2001-2002

E. Petit, A. Savalle, B. Jacquot, F. Chautard, P. Dolegieviez, P. Robillard, M. Ozille, M.H. Moscatello, F. Loyer, A. Peghaire

GANIL
Grand Accélérateur National d'Ions Lourds
Laboratoire commun CEA/DSM-CNRS/IN2P3

GANIL R 03 02

TECHNICAL REPORT ON OPERATING ACCELERATORS 2001 – 2002

Fig.1

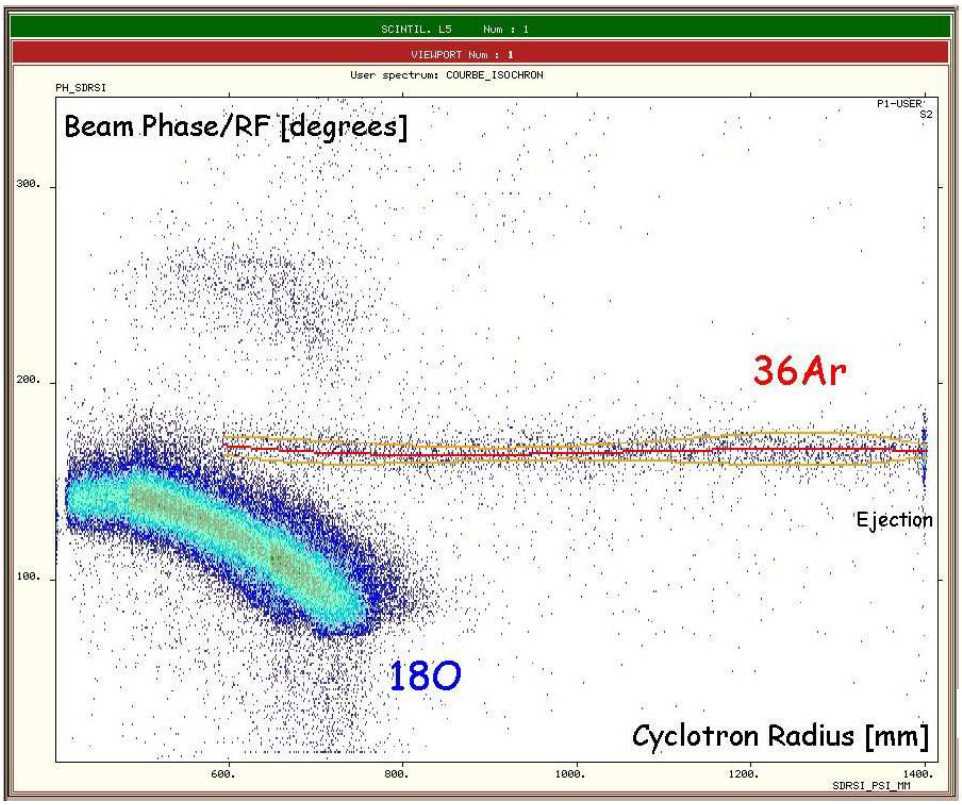

Fig.2

CONTENTS

Front page :
Fig1: Hydrogen target solid growth
Fig.2 : Phase measurement as function of the radius in CIME using a 300 µm silicon detector

FOREWORD

This issue of the Technical Report about the Accelerators describes the operation for physics experiments and beam tests, various technical improvements and projects for the years 2001-2002 during which the most eventful result was the start of the SPIRAL facility operation.

As usual the first chapter reports on the standard operation of GANIL with stable as well as radioactive beams, an analysis of the beam time distribution and statistics. Of course the most prominent event has of course been radioactive beams delivered for nuclear physics experiments. Then a status and an analysis of operation since 1996, with the evidencing of the increase of beam availability for physics experiments and the decrease of tuning time, are conveyed in this first chapter.

Beam tests were very numerous during these two years. In 2001, beam tests time were dedicated essentially to THI (beam instrumentation, understanding of THI beam power limitation to 3 kW) and to SPIRAL beam tests with radioactive beams. In 2002, less beam tests were planned during operation, nevertheless many tests with SPIRAL stable beam took place in parallel with operation for physics experiments. This is the content of the second chapter.

Technical studies, essentially concerning ion sources developments on stable and radioactive beams, are described in chapter 3.

During these two years THI project (chapter 4) carried on in the form of two projects called OPTHI and THI6K. OPTHI project allowed the routine operation of THI beams needed for the production of radioactive beams with SISSI and SPIRAL facilities, and also enabled the extension of THI beams for experimental areas. THI6K project, whose objective was to accelerate a 6 kW beam, proved the existence of longitudinal charge space effects in SSC2 limiting accelerated beam power. The decrease of the number of beam turns inside SSC2, in increasing the voltage of RF cavities, enabled the extraction of a 5 kW beam of ^{36}Ar.

The last chapter deals with a facility, called IRRSUD, which uses the low energy beams coming from the injectors. This new facility has been commissioned with beam and used for the first physics experiments in 2002. A status progress of the LIRAT project, which is a new very low energy radioactive beams line using beams produced with the SPIRAL Target and Source device and which will offer new possibilities for physics, can also be found in this last chapter.

Eric PETIT
Head of the Accelerator Division

.

PREFACE

Ce numéro du rapport technique des accélérateurs décrit le fonctionnement pour la physique, les études machine, les améliorations techniques et les projets pour la période 2001-2002 qui a été marquée par le démarrage de SPIRAL en faisceaux radioactifs.

Le premier chapitre décrit comme il est de tradition le fonctionnement des accélérateurs avec des faisceaux d'ions stables mais également radioactifs, l'analyse de la distribution du temps de fonctionnement et les statistiques. Le fait le plus important a bien évidemment été la fourniture de faisceaux radioactifs pour la physique nucléaire. Puis dans ce premier chapitre, un bilan et une analyse sont faits du fonctionnement des accélérateurs depuis 1996, avec la mise en évidence de l'augmentation du nombre d'heures faisceau fournies à la physique et la diminution des temps de réglage.

Les études machine ont occupé une place importante durant ces deux années. En 2001, le temps d'étude machine a essentiellement été consacré à THI (instrumentation de faisceau, compréhension de la limitation de la puissance faisceau à 3KW à l'éjection de CSS2) et aux tests de SPIRAL en faisceau radioactif. En 2002, moins de temps d'études machine a été programmé sur le temps de fonctionnement des accélérateurs, cependant en parallèle de la fourniture de faisceau à la physique de nombreuses études machine ont été dédiées à l'accélérateur SPIRAL notamment en faisceau stable. C'est l'objet du second chapitre.

Au chapitre 3 sont évoquées les études techniques qui ont essentiellement concerné les développements sur les sources d'ions aussi bien en faisceaux stables (ions métalliques) qu'en faisceaux radioactifs (études sur SIRA).

Le projet THI (chapitre 4) s'est poursuivi durant ces deux années sous la forme de deux projets appelés OPTHI et THI6K. OPTHI a permis la mise en exploitation courante de faisceaux THI nécessaires pour la productions de faisceaux radioactifs avec SPIRAL et SISSI, et a aussi permis l'extension de THI vers les aires expérimentales. THI6K, dont l'objectif était de parvenir à accélérer un faisceau de 6KW, a démontré l'existence de l'effet de charge d'espace longitudinal dans CSS2 limitant la puissance faisceau accéléré. La diminution du nombre de tours faisceau, en augmentant les tensions des cavités HF de CSS2, a permis d'extraire un faisceau d'^{36}Ar de 5.2 KW.

Le dernier chapitre décrit la fin de construction de la ligne basse énergie IRRSUD qui a été testée avec faisceau puis utilisée pour de premières expérience de physique durant l'année 2002. Ce dernier chapitre est également l'occasion de faire le point sur l'implantation au GANIL d'une nouvelle ligne d'ions radioactifs très basse énergie, appelée LIRAT, utilisant directement les faisceaux issus de l'ensemble Cible/Source de SPIRAL et offrant ainsi de nouvelles possibilités pour la physique.

Eric PETIT
Chef du Secteur des Accélérateurs

1

ACCELERATOR OPERATION

1.1 ACCELERATOR OPERATION in 2001 and 2002

A. Savalle

1 Highlights

2001

Two major failures occurred during the first two weeks, implying several days of intervention. The first one was related to the vacuum system of the rebuncher R1, while the second one was concerning the cooling system of SSC1 cyclotron.
After this period, the failure rate was normal and the experiments were carried out with no major difficulties.

During the second period, a high intensity ^{48}Ca (I>2.6 μAe corresponding to 400 W) was accelerated for three weeks. Despite the high intensity, the stability and the mean consumption were excellent.

In July, the first tests of the beam line L4 (which is used to transfer the beam towards the SPIRAL target-source) were made.
The administrative authorization needed was finally obtain in August. The two first SPIRAL beams were delivered to the experimental areas, in September and November : ^{18}Ne at 7 MeV.A and $^{8}He^{2+}$ at 15.5 MeV.A. To product this ^{8}He beam, the first THI beam (1 kW $^{13}C^{6+}$) was directed towards the SPIRAL target.

The THI project was pursued, and the difficulties related to high intensity beam dynamics overcome. Consequently, for the first time, a 5.2 kW beam ($^{36}Ar^{18+}$) could be accelerated.

2002

The accelerator operation started on March 11th, without any special difficulty.

Several SPIRAL beams (^{8}He, ^{6}He, ^{76}Kr, ^{74}Kr) have been accelerated at several energies.
The list is given bellow.

The primary beam intensity is, for the while, limited to 1.4 kW, for thermal reasons. In fact, in march , 2 target-Ion-Source-systems (TISS) broke, in presence of a beam power inferior to 1.3 kW. This failure was interpreted as a vacuum failure, due to thermal constraints on an alumina piece. After some mechanical modifications, a beam power of 1.4 kW was reached without difficulty. To enable the use of higher power beams (as 3 kW $^{13}C^{6+}$), the target itself is to be modified.

A major failure occurred in October : a water leak inside the RF cavity of SSC2. The intervention lasted for three weeks. During this period, the beam was delivered to SME and to IRRSUD, for technical tests.

The first irradiations with the IRRSUD beam line were realized in November 2002.

2. Accelerated beams

2001

1st period	ion	^{36}Ar	^{36}S	^{20}Ne	^{124}Xe	^{136}Xe	^{129}Xe	^{129}Xe	^{12}C	^{208}Pb
	Energy (MeV.A)	95	77.5	95	45	45	27	35	95	29
2nd period	ion	^{40}Ar	^{16}O	^{36}S	**^{48}Ca**		^{20}Ne	^{18}O		
	Energy (MeV.A)	5	13.7	50	**60**		95	63		
3rd period	ion	^{13}C		^{18}O	^{20}Ne		^{58}Ni	^{36}S		
	Energy (MeV.A)	60		63	95		75	77.5		
4th period	ion	^{13}C			^{36}Ar	^{86}Kr				
	Energy (MeV.A)	75			95	58				

THI Beams				
Ion	Energy (MeV/u)	Use	Beam Power (kW)	PPS
$^{36}S^{16+}$	77.5	SISSI (x2)	**1**	2.3 10^{12}
$^{20}Ne^{10+}$	95	Machine study	**3**	10 10^{12}
$^{48}Ca^{19+}$	60	SISSI	**0.6**	1.3 10^{12}
$^{58}Ni^{26+}$	75	SISSI	**0.8**	1.2 10^{12}
$^{13}C^{6+}$	75	SPIRAL	**1.4 (3 output SSC2)**	9 10^{12}
$^{36}Ar^{18+}$	95	Machine study	**5.2 (3 in operation)**	9.4 10^{12}
$^{86}Kr^{33+}$	58	LISE 2000	**0.66**	0.8 10^{12}

SPIRAL BEAMS		
Ion	Energy (MeV/u)	PPS
^{18}Ne	7	1. 10^{6}
^{8}He	15.5	1.3 10^{4}

2002

Ion	Energy (MEV.A)	Accelerator	THI
^{36}Ar	4.9	SSC1	
^{36}Ar	95	SSC2	
^{48}Ca	60	SSC2	0.55 kW
^{13}C	75	SSC2	1.3 kW
^{208}Pb	5	SSC1	
^{78}Kr	68.5	SSC2	0.65 kW
^{58}Ni	4.3	SSC1	
^{13}C	75	SSC2	1.4 kW
^{208}Pb	29	SSC2	
^{13}C	75	SSC2	1.4 kW
^{76}Ge	59	SSC2	
^{129}Xe	7	SSC1	
^{36}Ar	95	SSC2	
^{13}C	75	SSC2	1.4 kW
^{18}O	55	SSC2	
^{64}Ni	55	SSC2	
^{64}Ni	4.4	SSC1	

SPIRAL BEAMS		
Ion	**Energy (MeV.A)**	**Intensity (pps)**
^{8}He $^{1+}$	3.5, 3.4, 3.9	(5 to 8) x 10^{+4}
^{8}He $^{2+}$	13 15.7	2.5 x 10^{+4} 1.8 x 10^{+4}
^{6}He $^{1+}$	3.25	1.7 x 10^{+7}
^{6}He $^{1+}$	5	3.2 x 10^{+7}
^{76}Kr	4.4	1 x 10^{+6}
^{76}Kr	2.6	6 x 10^{+5}
^{74}Kr	2.6	1 x 10^{+4}

3 OPERATING STATISTICS :

2001

The time available for users decreased, due to waiting for the administrative authorisation for SPIRAL, the SPIRAL beam tests, and an important part of beam time dedicated to the THI machine studies.

Scheduled beam time distribution from 5 March to 16 December 2001		
	Hours	**%**
Preparation of beams	726	13.1
Nuclear Physics (HE)	3064	55.4
Non Nuclear Physics (HE)	286	5.2
Physics Tests	301	5.4
Machine beam tests	440	8.0
Waiting for Spiral authorisation	102	1.8
Spiral beam tests	276	5.0
Technical Interventions	224	4.0
Not defined	115	2.1
total	**5534**	100.0

Operation from 5 march to 16 december 2001

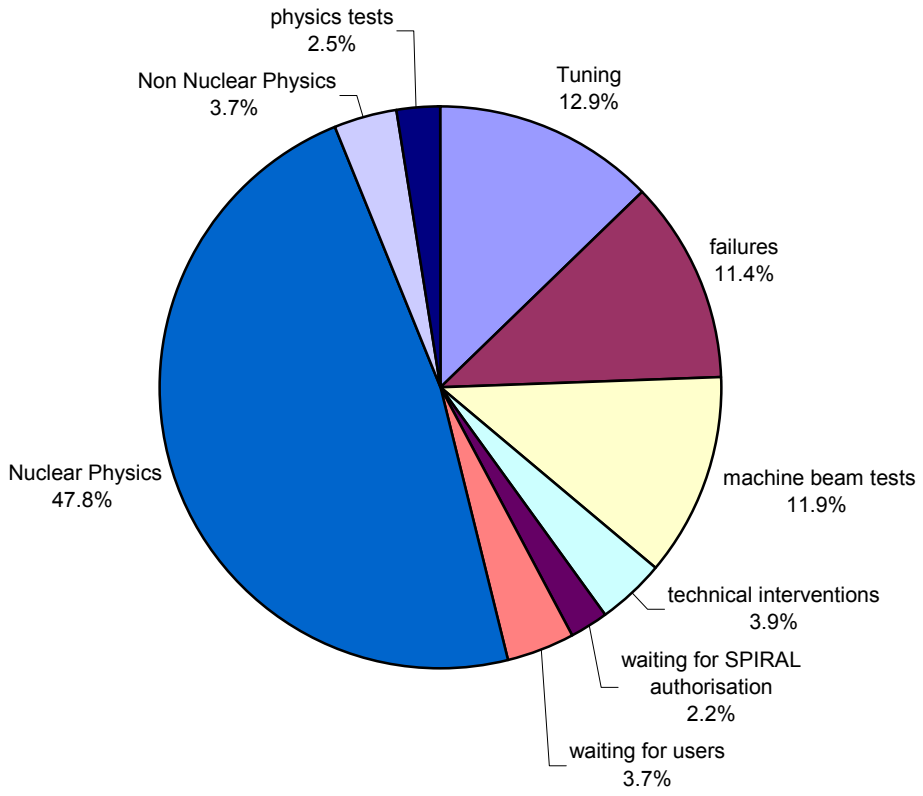

Beam time available for users = 57.7%

2002

The availability for users increased, due to an important decrease of the time allocated to machine beam tests.

Indeed, the main part of the accelerator development was dedicated to SPIRAL. These machine studies may generally be carried out using a CIME stable beam, while a SSC1 or SSC2 beam is available for physics.

Scheduled beam time distribution from 11th march to 20th December 2002		
	Hours	**%**
Security (UGS) tests	104	1.8
Preparation of beams	848	14.8
Nuclear Physics (HE)	3216	55.9
Non Nuclear Physics (HE)	450	7.8
Physics Tests	277	4.8
Machine beam tests	206	3.6
Not defined	648	11.3
total	**5749**	100.0

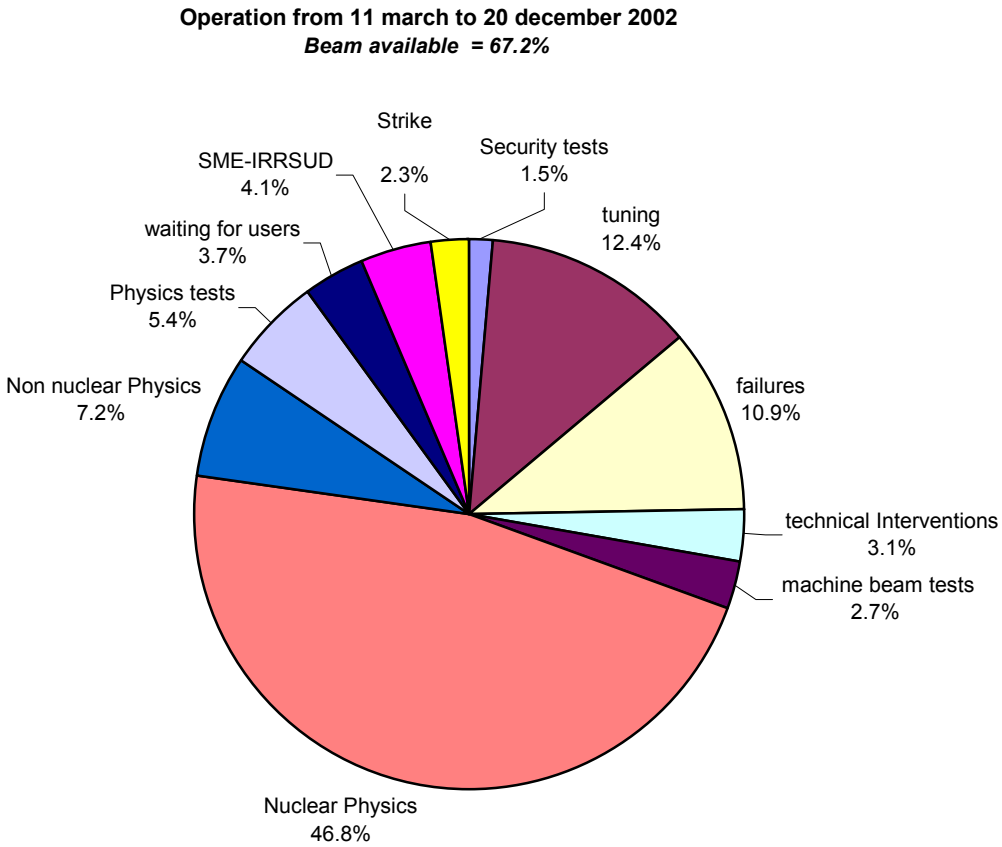

4 Failures Statistics

The distribution of the failures is the following :

2001	Hours	%
Power supplies	40.5	6.7
Electronics	8.25	1.3
Control-command	66.5	11.0
Logic controllers	12.75	2.1
R.F.	261.75	43.3
ECR Sources	62	10.25
SISSI	4	0.7
Cooling circuit	22.25	3.7
vacuum	52.25	8.6
Spr UGSR UGSA	25.25	4.2
Beam stops	9.5	1.6
Electricity	2.75	0.45
Other	37	6.1
total	**604.75**	100

Two important failures, related to R.F. equipment, occurred in march 2001.
The first one was related to the vacuum system of the rebuncher R1, while the second one was concerning the cooling system of the north cavity of SSC1 cyclotron.

2002	heures	%
Power supplies	78.75	13.78
Electronics	9	1.57
Control-command	3	0.52
Logic controllers	1.5	0.26
R.F.	92.75	16.23
Water leak RF SSC2	148	25.89
ECR Sources	3.25	0.57
Cooling circuit	15.25	2.67
vacuum	26.5	4.63
Security (UGSR, UGS2)	46.25	8.09
Beam stops	8.5	1.49
Electricity	3.25	0.57
ECS source	70.75	12.37
Other	65	11.37
	571.75	100

The cooling circuits of the RF cavity are the main cause of failure.
In addition to the water leak inside the RF cavity of SSC2, one has been encountered again on the north cavity of SSC1, while another was discovered on the dee of C02 injector. That dee has been totally rebuilt during winter 2003.
An important failure occurred, and is still present, concerning the main coil of CIME cyclotron (internal short-circuit). The characteristics of the main coil are changed, but not the working diagram of CIME.

1.2 EVOLUTION OF OPERATION SINCE 1996

A. Savalle

1 Beam availability and availability for physics

The availability for users was below 2500 hours in 1997-98, related to the construction of SPIRAL. Since then, the number of operation weeks has regularly increased (up to 35.5 weeks en 2002). Furthermore, the percentage of beam availability for users increased in 2002. Thus, the beam was used by physics during more than 3500 hours.

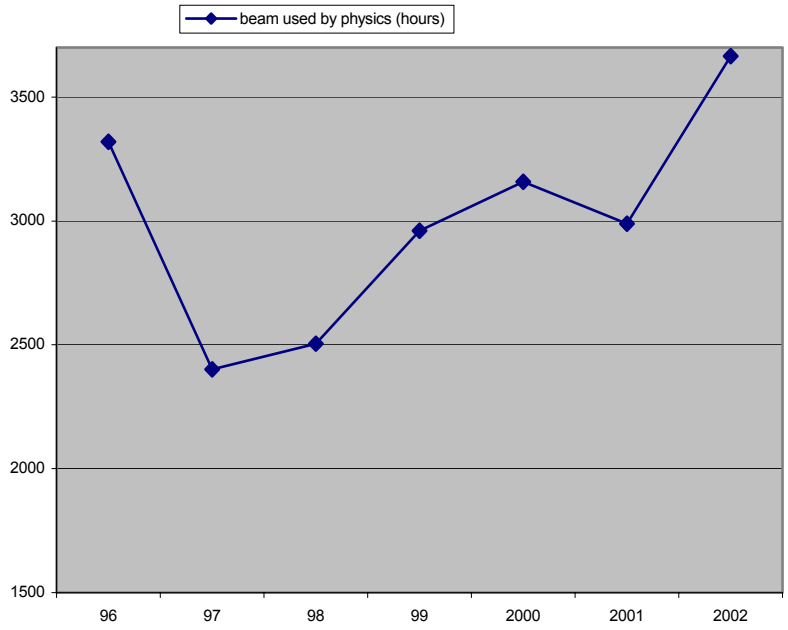

The beam availability includes, not only the availability for physics, but also the accelerator development. For example, the availability for physics is the lowest in 2001, due to the first SPIRAL tests and to major THI developments. However, the beam availability is higher in 2001 than in 1999, when several THI machine studies were cancelled.

Similarly, although the beam availability is not exceptional, the physics part is the highest in 2002. Indeed, the major part of the accelerator development has been made with a CIME stable beam.

Beam Availibility

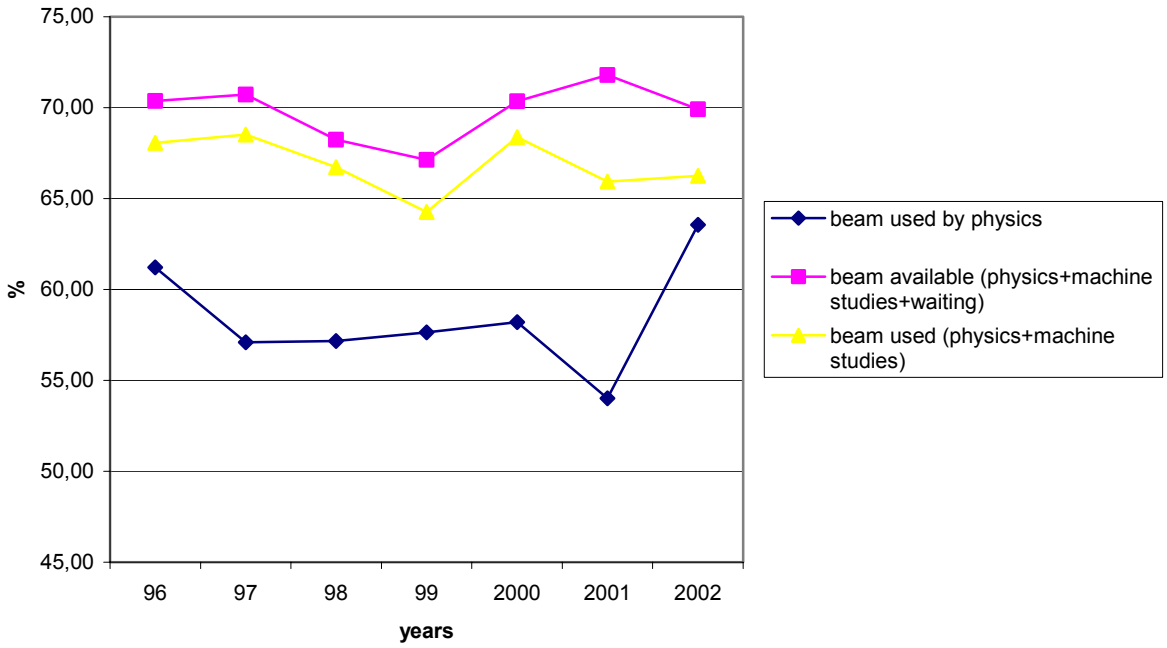

machine studies

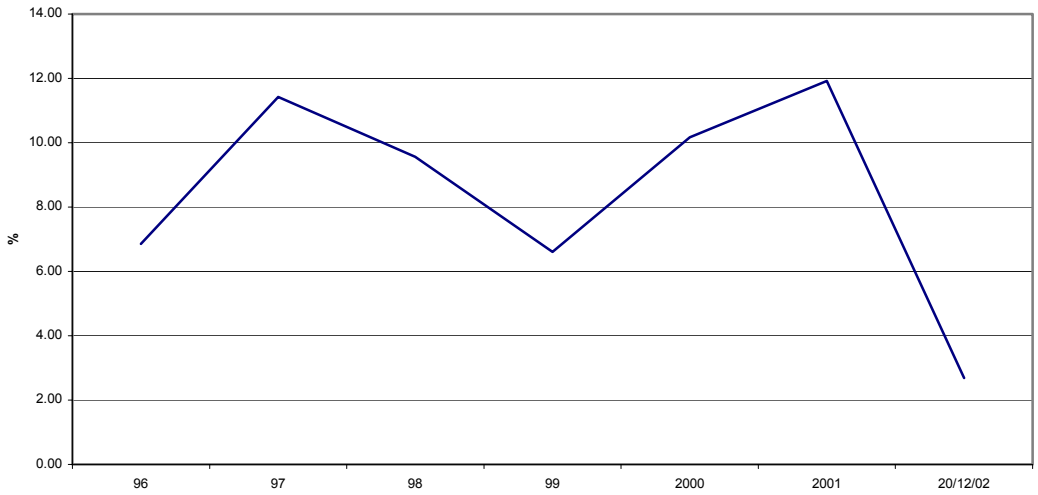

2 Evolution of tuning time

The tuning time is (in percentage) decreasing for several years.
First of all, note that this percentage is related to ratio (number of accelerated beams / number of operation weeks). In 1998, 28 beams were accelerated during 26 operation weeks. In 2001 and 2002, 25 beams have been accelerated during 35 weeks. This was obtained by grouping the experiments using the same beam together.
Nevertheless, an evolution can be seen from 1996 to 2002 (same number of accelerated beams). It can be explained by two ways :

- as far as SSC1 or SSC2 are concerned, the methods of tuning have been improved
- The CIME beams are planned so that the main part of the tuning is realized with a stable beam, while a SSC1 or SSC2 beam is delivered to physics. Similarly, the CIME stable beam may be used during the tuning of SSC1 and SSC2.

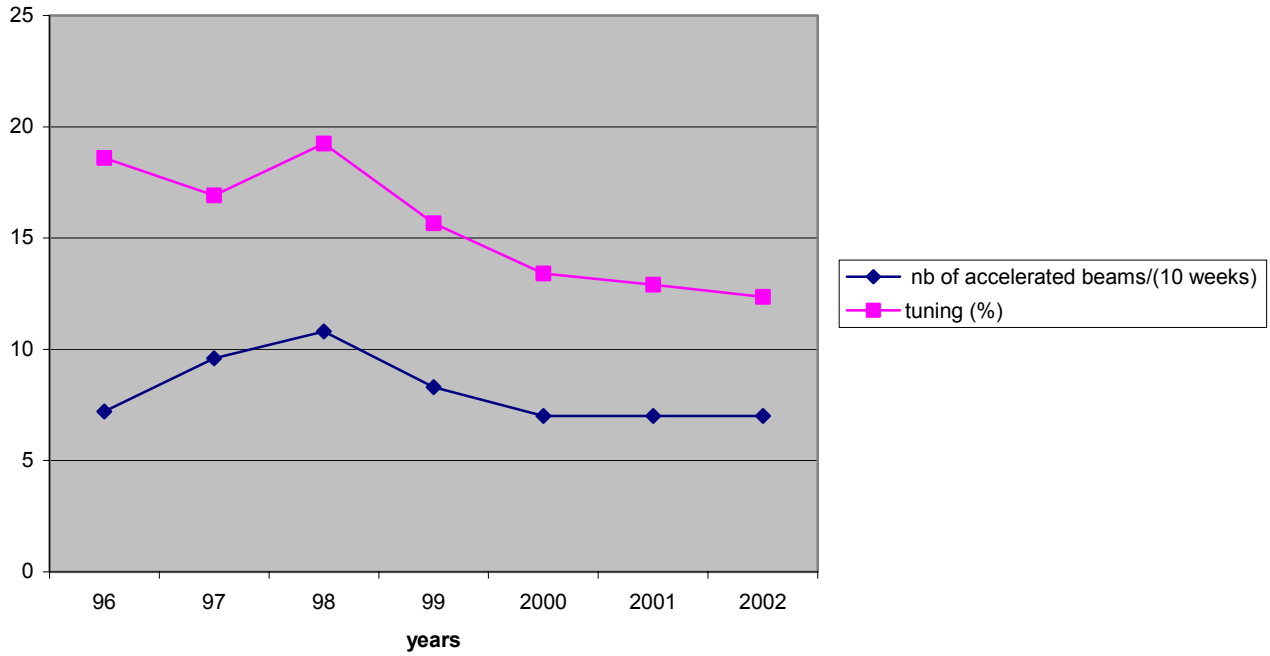

3 Evolution of failure rate

The failure rate has slightly increased for several years. A part of this evolution may be related to the number of equipments (SPIRAL). However, the several water leaks which occurred these last years are related to the age of the GANIL accelerator.

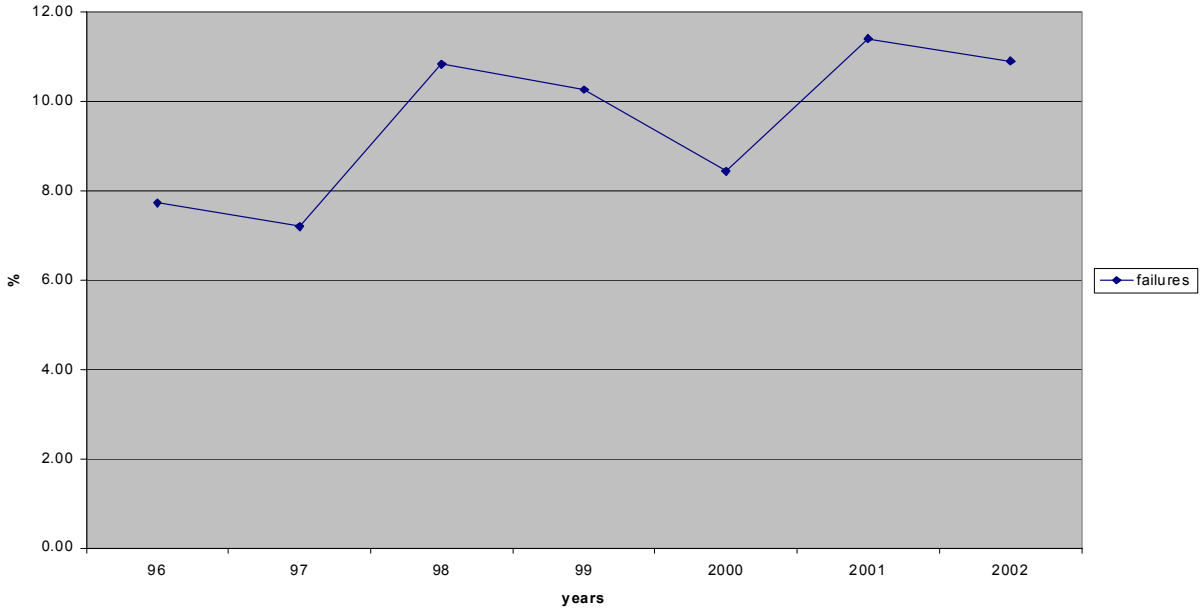

2
MACHINE STUDIES

2.1 MACHINE STUDIES in 2001 and 2002

A. Savalle

2001

12 % of operation time were devoted to machine studies, including the first SPIRAL tests with radioactive beam. The different subjects were :

- Beam instrumentation
- Automatic beam tuning

- THI :

The existence of longitudinal space charge effects in SSC2 was demonstrated. These effects were limiting the beam power to 2.5- 3 kW. It was shown that it was necessary to decrease the number of turns in SSC2, thus to increase the RF voltage. This voltage was increased up to 220 kV, in December 2001, and a 5.2 kW beam power was produced ($^{36}Ar^{18+}$ beam).

  - Study of the beam dynamics in C01 injector
  - Study of the effect of the transverse emittance
  - Development of digital feedbacks to stabilize the beam

- SPIRAL :

  - Study of the CIME (stable) beam characteristics in the "Z" spectrometer
  - test of the beam line L4 : a ^{20}Ne beam, at 95 MeV.A, then a ^{13}C beam at 75 MeV.A, were directed to the Target-Ion-Source-System (TISS), through the beam line L4. The aim was to check the equipment, the transmission, the beam width on target.

  - Test of SPIRAL TISS

  - Test of the low-energy Identification station, and of the CIME instrumentation for radioactive beam

  - Test of the tuning method for radioactive beams, by extrapolation of a stable beam of similar q/A.

2002

2.7 % (130 hours) of operation time were dedicated to machine studies :
- Tests of THI security system.
- Beam instrumentation
- Automatic beam tuning
- Study of the beam dynamics in C01 injector
- Irradiation of a copper target, to measure the activation
- Measurement of the production rates of several beams, with the SPIRAL low-energy Identification station

These 130 hours have needed an interruption of beam delivery to physics. In addition, 250 hours have been dedicated to machine studies using a CIME stable beam. The different subjects were :

- Study of the TISS extraction

The extraction optics depends on the extracted ions and on the intensity. Moreover, a misalignment defect is present (estimated to 1 cm at the output of the einzel lenses). The tuning of the injection beam line (from TISS to CIME) is complicated by these two phenomenon.

- Tuning methods from stable beam to exotic beam

Two methods may be applied : change of the magnetic field level or change of the RF frequency, according to the formula : $B*R = \gamma mv/q$. Using anyone of these two methods, the difficulty is higher at high energy (harmonics 2 and 3) than at low energy (harmonics 4 and 5). It can be explained by two facts : the number of turns which is higher in harmonics 2 and 3, and the relativistic factor γ which can not be neglected at high energy. The consequence is that an empiric re-tuning of CIME ejection, from stable to exotic beam, is necessary.

- Continuous frequency shift

The possibility to change continuously (without stopping the high voltage) the CIME RF frequency has been checked. The aim is to accelerate successively different ions of similar q/A, for precise mass measurements.

- Change of energy

Some experiments use beams at several energies. A change of energy, at the output of a cyclotron, is generally considered as a complete new tuning. However, it has been proved that it is possible, by extrapolation, to realize a change of CIME energy of 10 to 20% in about 1 UT (8 hours).

- Extension of CIME working diagram with the two centers

Two different centers (inflectors, RF cavity noses) are used in CIME, depending on the injection radius : 34 mm for harmonics 2 and 3, 45 mm for harmonics 4 and 5. It has been demonstrated that it is in fact possible to accelerate a beam in harmonics 4 with h2-h3 center, and to accelerate a beam in harmonics 3 with h4-h5 center (in that last case, a limitation exists on the energy due to the source voltage).
Thus, the number of interventions to change the CIME center can be limited (1 day is necessary for this intervention, not including possible waiting due to activation of the center).

2.2 SPIRAL
Beam optics studies & Accelerator operation

B. Jacquot

The availability of SPIRAL cyclotron, "CIME" , during GANIL experiments has permitted the feasibility of a lot of beam optics studies. We recall the principle of the tuning of the cyclotron with radioactive ion species and summarize few results about the cyclotron and beam line studies, mass selection, and software development for the operation of the SPIRAL Facility.

I) Cyclotron Operation with radioactive ion species

Principle

Owing to the very low intensity of the exotic beams, it is very hard to tune the cyclotron directly with the beam of interest. That is why, the tuning is realised with a stable isotopic beam delivered by the ion source. If a specific element is needed for that tuning, we can inject it in the source from a gas bottle. The intensity available with this stable element allows an easy tuning and the optimisation of each accelerator section.
Then, the challenge is to perform, in a blind way, a scaling of the accelerator parameters to extract the very low intensity radioactive beam out of CIME and conduct it toward the experimental areas.

Strictly speaking, the only way to reproduce the same trajectories with the radioactive beam as the ones of the stable beam used for the tuning is to scale all the electric fields and magnetic fields with the factor c (strategy a):

$$c = \frac{M_1 Q_2}{Q_1 M_2} \qquad \text{(I.1)}$$

This corrective factor applied on all the fields implies the conservation of the Newton-Lorentz equation.

Practically, the modification of all the equipments is not necessary especially if the mass over charge ratio of the two ions are very close. Moreover such a global scaling is not desirable for the convenience and the operation reproducibility.
Mainly, two simplified strategies can be defined to adjust the accelerator parameters to the radioactive beam after the tuning:
-Strategy b : a RF frequency shift
-Strategy c : a magnetic field scaling
We explain below the two strategies : A given ion, with a mass M_1 and charge Q_1, performs one turn in the cyclotron with a fixed frequency f_{rev}:

$$f_{rev} = \frac{Q_1}{2\pi M_1} \frac{B(r)}{\gamma} \qquad \text{(I.2)}$$

where γ is the relativistic factor. To be accelerated properly in a cyclotron, this ion species has to stay in phase with the RF accelerating cavities during all the

acceleration. Therefore the magnetic field B has to be tuned to ensure the synchronism between the RF system and the ion revolution, such as:

$$f_{rev} = f_{RF} / H \qquad \text{(I.3)}$$

Where H is called the harmonic.

In the figure 1, the beam n°1 stays in phase with RF accelerating cavities while it is not the case for the beam n°2, we have

$$\frac{Q_2}{2\pi M_2} \frac{B(r)}{\gamma} \neq \frac{f_{RF}}{H} \qquad \text{(I.4)}$$

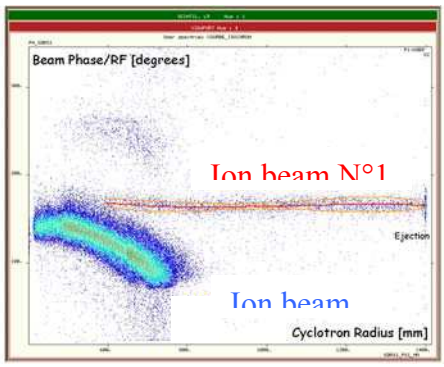

Fig. 1: Phase measurement as function of the radius in CIME using a 300 µm silicon detector. Test realised with ^{36}Ar (ions n°1) and ^{18}O (ions n°2) on harmonic 3.

Let us note that by adjusting either the RF frequency or the magnetic field, the beam n°2 could fulfil the synchronism condition and thus be accelerated up to extraction of the cyclotron: This is the basic principle of the cyclotron's tuning.

Hence, after the tuning of stable ion species, we can use either the magnetic field or the RF frequency to shift towards the correct tuning for the radioactive beam (or a combination of both).

It is hard to monitor large modifications of the magnetic field level, since it modifies the global configuration of the field inside the cyclotron, this effect would alter the isochronism. Furthermore, magnetic field variations are not completely reversible, and another strategy is most of the time

preferred. Although the frequency shift (strategy b) can be realised with an accuracy below 10^{-7}, a large modification of the frequency, which is needed to accelerate radioactive ions with a rather different mass over charge ratio, induces a modification of the revolution frequency at large radius. This isochronism defect is a pure relativistic effect coming from the radial dependence of γ factor :

$$\gamma = \left(1 - \frac{(2\pi f_{rev} r)^2}{c^2}\right)^{-1/2} \qquad \text{(I.5)}$$

The isochronism, which guarantee optimum transmission, is altered. Therefore to restore the equality in eq.(I.4) over the whole acceleration process, B(r) should be theoretically modified with an accuracy around 10^{-5}, which is not easy. So, it is important that the mass over charge ratio of the stable element used for the tuning is not too far from the desired radioactive ion in order to perform frequency shift which do not alter too much the isochronisms.

Numerous studies have demonstrated that the RF frequency shift (strategy b) is the most convenient and reliable method to pass from the tuning ion beam toward the radioactive ion beam. In harmonics 4 and 5 (2-6 MeV/A), the radioactive ion beam is ejected directly from the cyclotron after the frequency shift. For harmonics 2 and 3 (5-25 MeV/A), the ejection of radioactive beam is much more difficult since the large turn number coupled to a slight precession and to the relativistic effects make the trajectory of the radioactive beam different from the tuning beam. The case of $^{8}He^{2+}$ at 15 MeV/A is the worst as we explain below.

Difficulties with $^{8}He^{2+}$

Difficulties have been encountered in the very peculiar case of the acceleration $^{8}He^{2+}$ around 15 MeV/A. Several reasons make it very difficult to extract $^{8}He^{2+}$ from the cyclotron. We summarize the different origins of the difficulties :

1) The tuning has to be realised with a stable element whose mass over charge ratio *M/Q* is not to far from the one of $^{8}He^{2+}$. In that we case, we have to choose $^{16}O^{4+}$ which is polluted with a $^{12}C^{3+}$ ion beam and can prevent us to tune properly the cyclotron.

2) The emittance of helium ion beam in the low energy beam line can reach up to 150 π mm.mrd which is the worst case for the ECR ion source, leading to very poor transmission of the accelerator (10-15%).

3) The most convenient strategy to pass from the stable ion beam to the radioactive ion beam is the RF frequency shift. This strategy is not exact since the two ion beams will not describe strictly the same trajectory because of relativistic effect which become non negligible at 15 MeV/A. The difference between the two trajectories make the transmission at the extraction of the cyclotron very different for the stable ion beam and the radioactive ion beam. It can occur that all particles get lost in ejection channels, imposing to search randomly the value of the 9 parameters of the ejection. As a result, the tuning time needed should be increased to adjust properly the ejection of the cyclotron.

A large part of the beam time allocated to the accelerator studies has been devoted to the understanding of the different problems. We have established that a minimization of the precession in the cyclotron and a perfect tuning of isochronism are of utmost importance to be able to eject $^{8}He^{2+}$ with a good transmission in harmonics 2.

Mass purification

As far as the purification of very rare isotope is concerned the achievement of very good mass resolution is not sufficient. Since stable contaminants can dominate by several orders of magnitude the intensity of given radioactive ion species, it is of utmost importance to perform a very clean separation.

A given ion, with a mass M_1 and charge Q_1, performs one turn in the cyclotron with a fixed frequency f_{rev}. When the synchronism condition is fulfilled, the relative phase ϕ_1 of the ions with the RF accelerating cavities stay constant altogether with the energy gain per turn ΔE^{1}_{turn}, which is given by

$$\Delta E_{turn} \propto V_{RF} \cos(\phi_1) \qquad \text{(I.6)}$$

The ions are thus accelerated up to the ejection channel of the cyclotron. For another ion, with a different mass to charge ratio (M_2/Q_2), the synchronism condition is not fulfilled, the relative phase ϕ_2 with the RF system evolves up to ϕ_2=90°, and then these ions are not accelerated anymore ($\Delta E_{turn} \le 0$) and get lost inside the cyclotron (see for instance Fig. 1, ions N°2). This mechanism allows the elimination of any undesired ion if the mass over charge ratio is such that its phase exceeds 90° before the end of the cyclotron. This condition corresponds at first order to:

$$\left[\frac{M_2}{Q_2} - \frac{M_1}{Q_1}\right] \Big/ \frac{M_1}{Q_1} < \frac{1}{2\pi H N_{turn}} \qquad \text{(I.7)}$$

where N_{turn} is the number of turns. Hence the mass resolution of a cyclotron is defined as $R = 1/2\pi H N_{turn}$. Depending on the harmonic, the mass resolution of CIME can reach 1.6 10^{-4}.

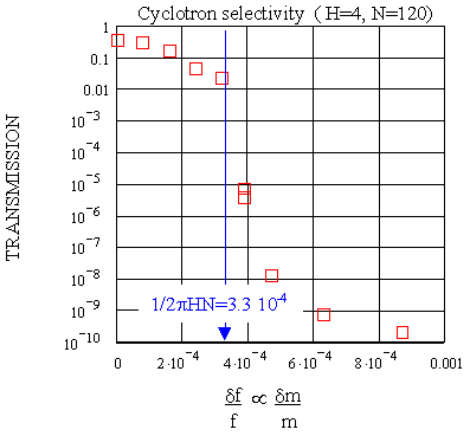

fig.2 : Transmission of CIME cyclotron as a function of the mass over charge ratio deviation.

The mass selection obtained experimentally, whatever the harmonic, is close to the one expected theoretically (fig 3). Besides the cyclotron ensure a very clean separation, since the ion contaminants with mass deviation greater than 5.10^{-4} are strongly suppressed : the transmission for these ions are smaller than 10^{-6}.

This study demonstrate that the nominal tuning, associated with the selectivity of the ECR ion source allow a total purification, provided that the charged state of radioactive ions are properly chosen. In the context of SPIRAL2, heavier ions (A>100) produced by non-chemically-selective sources could be accelerated with CIME. A much better mass resolution will be required to purify the beams. The possibility to achieve a resolution around 5.10^{-5} would be studied very soon.

II) Beam line studies

Low energy beam line

Since the beginning of the SPIRAL operation, very large misalignment defects at the source extraction have been reported. During the first test period (2000-2001), several off-line beam's reconstruction has confirmed a deviation of 10-20 mm from the axis in the horizontal plan at the exit of electrostatic lenses. Such a large misalignment prevent us to optimize the matching of radioactive ions at source extraction with the electrostatic Einzel lens which induced additive misalignment when corrections are applied. This fact is a strong limitation in operation since it is really important for the transmission of radioactive ions to match exactly the stable beam used for the tuning.

The origin of the misalignment has not been perfectly determined. Nevertheless, the magnetic fringe field of the source sextupole at the extraction region could explain such deviations. The replacement of the source system for each experiment does not allow to correct such a defect with a re-alignment of source system.

Therefore two additive steerers will be added in the beam line to compensate the large deviations observed.

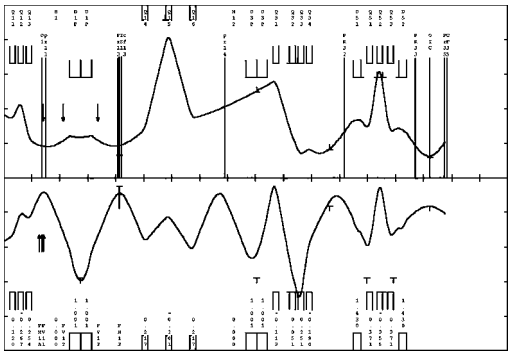

fig 3: Beam envelop reconstruction with Transport program in the low energy beam line *($\varepsilon x = \varepsilon y = 120\pi$ mm.mrd)*

Medium energy beam line (CIME ejection)

While we could expect theoretically at the exit of the cyclotron a transverse beam emittance of 5-10 π mm.mrd, we often observe an emittance around 40 πmm.mrd in the horizontal plane. Such a large emittance figure could induce large beam loss in the Z spectrometer and is not suitable for a lot of physics experiments.

Actually, the beam envelop is dominated by a chromatic effect, indeed, particles with different momentum will not follow the same trajectory, increasing a lot the size of the beam. Let us underline that the dispersion vary a lot from one setting to another since the whole energy range of the cyclotron is quite wide (from 1.7 to 25 MeV/A). Therefore the momentum dispersion is still not perfectly known, and the computed optics of the medium energy line do not permit the compensation of momentum dispersion. The measurement of the momentum dispersion is far from obvious and do not allow to re-compute easily the optics to correct the defect, and on-line adjustments are needed to minimize the beam size.

Tedious optimization of quadrupole settings permit to reach 15-20 π mm.mrd in the horizontal and the vertical plane.

Efforts have been made to decrease the tuning time and guarantee the reproducibility of the operation. A software has been develop allowing the fast optimization of the beam intensity in a given emittance.

III) SPIRAL operation with new softwares

The operation of SPIRAL accelerator and beam lines has benefited from the development of large number of software components for GANIL accelerator. Indeed, lot of time consuming tasks can be realised in-line automatically (beam centring, betatron matching, isochronisms, achromaticity) thanks to different beam detectors (profile

monitors, beam central phase probes,…) and the associated control system. Most of software programs have been adapted for the operation of SPIRAL, but the specificity of the CIME cyclotron and new scientific request leads us to upgrade and develop new software programs.

Computer aided on-line optimisation

The tuning of SPIRAL is generally a time consuming task, since optimum transmission is required with the scarce radioactive ions. During the first year of SPIRAL, we realized that the time needed to optimize beam transmission through the accelerator is hardly compatible with the different operational constraints. The good transmission figures in the cyclotron have been obtained after careful tunings and painful optimizations.

A new computer program based on a steepest descent algorithm has been developed. Object programming concepts have been implemented to open up the possibility to optimize any function of different beam diagnostics with a large variety of equipment. The basic algorithm can be summarized as follow :

-Start with set of accelerator parameters (P1,..PN) and measure on a diagnostic the function to optimise I(P1,…,PN), typically a beam intensity.

- Compute the gradient ∇I(P1,…,PN) ,by measuring successively $I(P1+\varepsilon,\ldots,PN)$, …. $I(P1,\ldots,PN+\varepsilon)$.

- Search the optimum in the direction of the gradient ∇I(P1,…,PN). And restart with the new set of parameters (P1',…,PN').

An important literature is devoted to the mathematical problem of function's maximisation (or minimisation). For instance, we can ensure a better convergence of the algorithm by an orthogonalisation of the successive directions of optimization (conjugate gradient method in multidimension). Let us underline that the mathematical details of the optimization to speed up the convergence are less important in this context than the robustness of the algorithm. One of the main problem is to get reliable measurements. Averaging with several measurements in order to smooth non-significant fluctuations is needed. Moreover, the increments ε to be applied on the set of accelerator parameters should be carefully chosen to compute the gradient ∇I(P1,…,PN).

The implemented algorithm allows the optimization of the beam's transmission beam at the injection of the cyclotron with 20 parameters within 3 minutes. We use it to optimise the cyclotron ejection region, and also to decrease the chromatic horizontal emittance in the medium energy beam line. Let us note that the optimization stage do not replace the tuning stage but permit us to get better transmission, and a better beam quality in a reasonable time interval.

"Fast" Energy variation

Different physicist requests have underline the scientific interest to change as fast as possible the energy of the beam downstream of the cyclotron. Conversely to a tandem or a linac, the energy variations with a cyclotron like CIME are really difficult since all the magnetic fields, electric fields and RF frequency of RF cavities have to be rescaled.

The tuning of the cyclotron and beam lines for a given ion beam at given energy required 16-24 hours. Starting from beam well tuned in the cyclotron, we aim to modify the set-up in order to accelerate the same beam with a slight different energy (±20%) within 4 hours. Generally, a set of theoretical cyclotron parameters P_{theo} (M_1,Q_1,E_1) computed to accelerate an ion beam (M_1,Q_1) at the energy E_1 has to be adjusted empirically to deliver the beam with good transmission. The difference $\Delta P_{Theo-Exp}$ between the theoretical parameters and the experimental ones take account of the hysteresis in the magnet, temperature, misalignment, equipment defect.

The extrapolation of the cyclotron tuning from one energy to another is performed as follow

$$P_{Exp}(M_1,Q_1,E_2) = P_{theo}(M_1,Q_1,E_1) + \Delta P_{Theo-Exp}(E_1) .$$

Numerous tests have been realized and it appears that energy variations can be realized rather quickly, within 4 hours. A loss in transmission around 50% is, nevertheless often observed. If an optimum transmission should be recovered, 8 hours has to be spent.

The developed software performs the extrapolation task of the tuning parameters from one ion beam (M_1,Q_1,E_1) toward another ion beam (M_2,Q_2,E_2). Besides the software has been implemented also to handle the different strategies to pass from the tuning ion beam toward the radioactive ion beam as explained in chapter I.

CONCLUSION

The most remarkable result with the cyclotron is the good transmission in the whole energy range, from 1.7 to 25 MeV/A (Tab.1).

H (Har-monic)	Number of turns	Transmission with stable ions	Beam quality
2	330	~ 30%	$\varepsilon x \sim 15\pi$m m.mrd $\frac{\Delta E}{E} < 0.005$
3	280	30-40%	
4	120	30-35%	
5	100	15-20%	

Tab. 1: Cyclotron transmission, for beams included in 80 π mm.mrd.

During the first year operation of Spiral with radioactive beams, our efforts have been

focused to improve our ability to deliver any ion beams with a good accelerator transmission with a correct beam quality within a reasonable time interval.

Some works is still needed to improve our flexibility in the delivery of different ion beams.

Several aspects will need more work to improve the beam qualities: a systematic study in the whole energy range of the cyclotron is still required for the understanding of the chromaticity in the medium beam line which is related to the observed horizontal emittance. Besides better understanding of the beam's matching in the injection line will be necessary to improve the beam quality.

2.3 Energy range extension of the CIME centres

F. Chautard

Introduction

The cyclotron CIME has an axial injection system, which let the possibility to accelerate ion beams from 1.7 to 25 MeV/u at the RF harmonics[1] H=2,3,4,5. However, two different centres are needed to cover such a large energy range:

The low-energy beams, from 1.7 to 6.2 MeV/u, are injected at a radius R=45 mm, using a Pabot-Belmont inflector, and accelerated on RF harmonics 4 or 5 (fig 1).

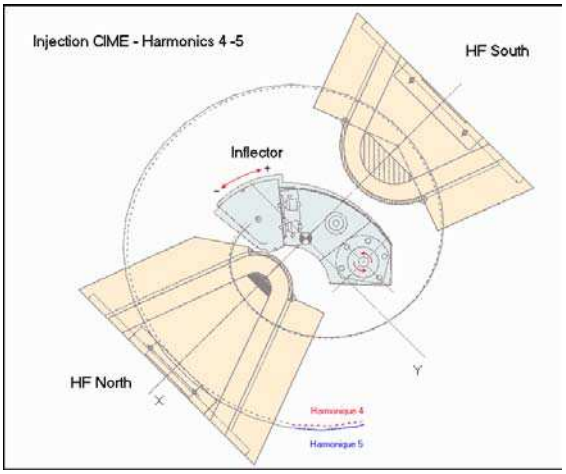

Figure 1: CIME central region for the harmonics 4 and 5. Composed of two RF extremities and a SPIRAL inflector followed by an electrostatic quadrupole. The trajectory of a reference particle is depicted.

The High-energy beams, from 4.9 to 25.4 MeV/u, are injected at a radius R=34 mm, using a Muller inflector complemented by an electrostatic quadrupole and accelerated on RF harmonics 2 or 3 (fig 2).

[1] Radio-Frequency Harmonics : ratio between the frequency of the acccelerating cavities and the ion revolution frequency in the cyclotron. Practically, the Harmonics corresponds to the number of ions bunches per turn in the cyclotron.

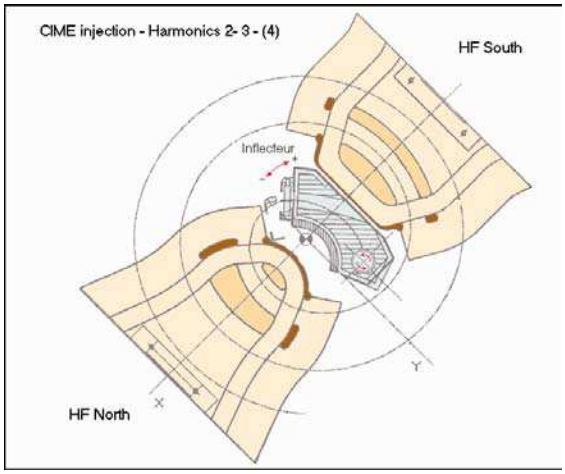

Figure 2 : CIME central region for the harmonics 2 and 3. Composed of two RF extremities and a MULLER inflector.

For the two energy domains, special dismountable extremities of the RF cavities have been designed to optimise the transit time at the injection.

The exchange of these two centres, inflector and RF cavities extremities, requires a 2 days intervention. This time consuming task represent an additive operational constraint of SPIRAL. Practically, we cannot deliver successively a high energy beam and a low energy beam during the same SPIRAL run. Moreover, in the context of Spiral2, the strong activation of the inflector could forbids any handling during long period. Therefore, there is a strong interest to enlarge as much as possible the energy range of each centre.

Simulations have been undertaken to evaluate the parameters which allow the injection and the acceleration of the beam in the cyclotron centre. These simulations allowed the determination of the beam injection energy. Then, the platform voltage and the magnetic rigidity (Bρ) of the transport line can be deduced. Values of the isochronism coils are computed with the suitable centre considering that the isochronism law is identical for a given frequency (same beam energy) and field level.

The value of the two first isochronism coils, B1 and B2, which determine the magnetic field in the cyclotron center are not obvious to evaluate. A careful multiparticle simulation help us to compute the optimum magnetic field configuration.

Given that the geometry of RF cavity extremities is different from one centre to another (fig. 1 and 3), the values of these 2 coils have to be modified. Hence, the value of the two first isochronism coils are adjusted as a function of the field level and the RF harmonic, to bring the beam in phase in the first cavity gaps.

1. Acceleration in H3 with the "45 mm centre"

Preliminary simulations have shown that it was possible to accelerate a beam under these conditions. It is possible, from parameter values of isochronism coils and the main field computed for the harmonic 3 with the centre 34 mm, to accelerate a beam with the centre 45 mm. Simulations show the necessity to increase RF voltage to accelerate the beam through the first gaps. The maximum voltage of the RF cavity and the source platform represent the limitation to extend the limits of this centre towards the high energy (fig. 3)

The test performed with $^{16}O^{4+}$ Ion beam at 6.0 MeV/A have been successful. CIME yields with opened emittance slits (> 200 pi.mm.mrad) are correct.

Yields obtained after 4 hours tuning (see parameters in Annexe):

IC_CF13	IC_CF35	IC_CF81	L5_CF11
[μA]	[μA]	[μA]	[μA]
1,63	1,33	1,2	0,40

The yield between the injection and the CIME ejection is 33 %.

2. Acceleration in H4 with a "34 mm centre"

To complete the study, we have to evaluate the acceleration of a beam in harmonic 4 injection centre initially dedicated to the harmonic 2 and 3. The simulations allowed the determination of the injection energy at 34 mm. It is possible, from parameter values of the isochronism coils and the main field computed for the harmonic 4 with the centre 45 mm, to accelerate a beam with the centre 34 mm.

The test performed with $^{40}Ar^{6+}$ ion beam at 5.18 MeV/A have been successful.

Yields obtained after a 4 hour tuning :

IC_CF13	IC_CF35	IC_CF81	L5_CF11
[μA]	[μA]	[μA]	[μA]
0.650	0.632	0.557	0.205

The yield between the injection and the CIME ejection is **31 %**. The yields of CIME with opened emittance slits (> 200 pi.mm.mrad) are in the order of the optimum tuning with the other injection centre.

Let us mention that a limitation exists : We cannot reach with this injection radius the very low energy region since it would need a very low injection energy. The minimal source platform voltage has been arbitrarily fixed to 10 kV. Below this value, the space charge effect becomes non negligible and important beam quality degradations would alter the beam transmission. Therefore only a fraction of the energy in H4 as a function of the Q/A is accessible (fig. 4).

3. General Conclusions

It has been shown that it is possible to reduce the number of change of centre with equivalent efficiencies. The Figure 5 shows that all accelerated beams up to now might have been accelerated with a centre H2-H3 and a voltage platform between 34 kV and 8 kV.

In the next year, the possibility to accelerate the beam in the harmonics H=6 will be studied to enlarge the energy range toward the low energy (> 1.2 MeV/u).

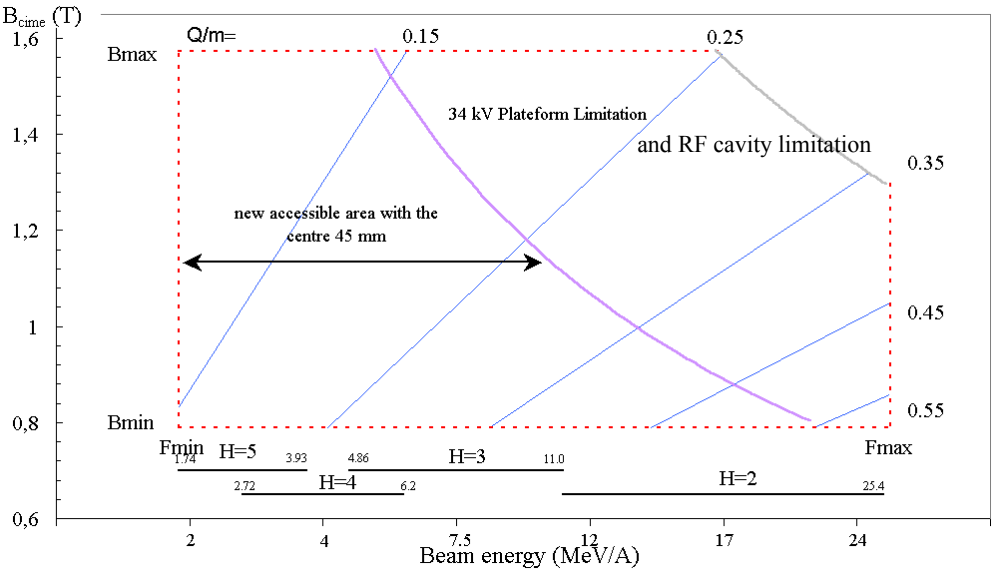

Figure 3 : New accessible energy range with the centre H4-H5

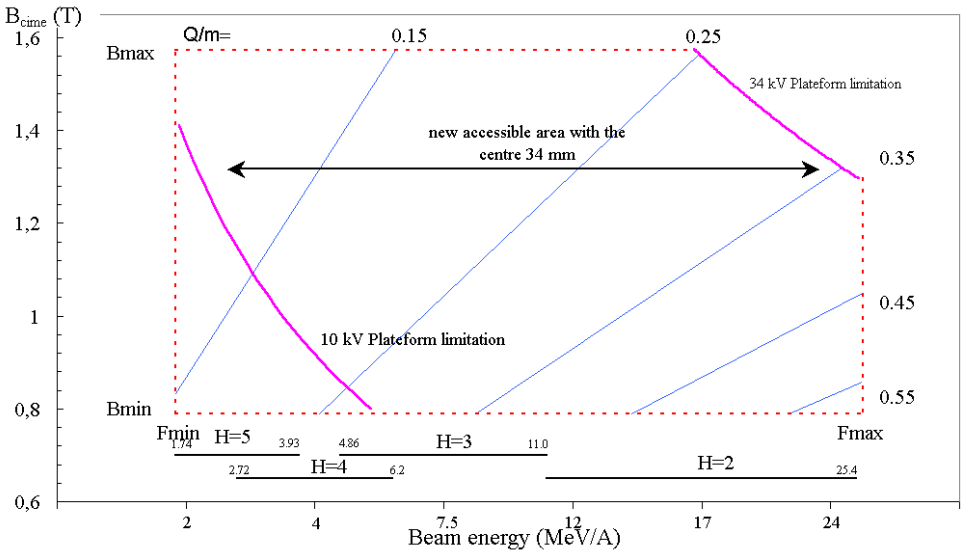

Figure 4 : New accessible energy range with the centre H2-H3

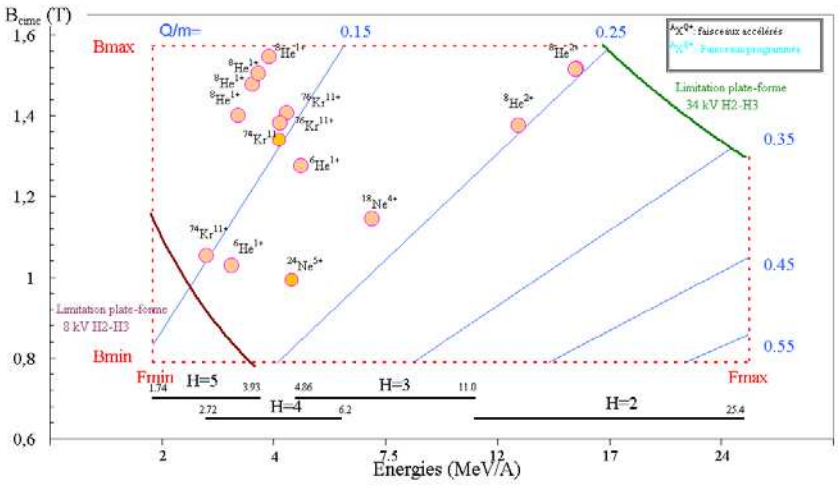

Figure 5 : SPIRAL beams accelerated from November 2001.The min max limitation of the platform voltage are plotted.

Annexe: Simulation's result

For historical reasons simulations with the program `lions` (*ref : GANIL R 93 08*) must be done at a beam revolution frequency of 4.8 MHz. Which corresponds to 14.4 MHz for H3 and 19.2 MHz for H4.

A) Acceleration in H3 with the "45 mm centre"

<u>According to the simulations at 14.4 MHz and H3:</u>

Ion : $^{16}O^{4+}$, Q/A = 0.25
Injection energy = 10.73 keV/A
Source voltage = 16 * 10.73 / 4 = 42.9 kV
Cavity voltage = 85000 V

From these calculated parameters we choose a beam of interest in the frequency range.

<u>Beam and parameters selected :</u>
Ion : $^{16}O^{4+}$, Q/A = 0.25; H = 3
RF Frequency = 10.66 MHz
Injection energy = (FHF/14,4)**2 * 10.73 = 5.88 keV/A
Source voltage = (FHF/14.4)**2 * 42.9 = 23.52 kV
CIME ejection energy = 6 MeV/A
Transport line (TBE) magnetic rigidity = 0.04415 T.m
RMN value at the CIME north sector = 12213 G (BP = 931 G)
Cavity voltage = (10.66/14.4) * 85000 = 63 kV

B) Acceleration in H4 with a "34 mm centre"

<u>According to the simulations at 19.2 MHz and H4 :</u>
Ion : $^{40}Ar^{6+}$, Q/A = 0.15
Injection energy = 5.814 keV/A
Source voltage = 40*5.814/6=38.7 kV
Cavity voltage = 83300 V

<u>Beam and parameters selected :</u>
Ion : $^{40}Ar^{6+}$, Q/A = 0.15; H = 3
Frequency FHF = 13.22 MHz
Injection Energy = (FHF/19.2)**2 * 5.814 = 2.75 keV/A
Source Voltage = (FHF/19.2)**2 * 38.7 = 18.4 kV
CIME ejection energy = 5.187 MeV/A
Magnetic rigidity = 0.0503 T.m
RMN value at the CIME north sector = 18955 G
Cavity voltage =(FHF/19.2)*83300=57 kV

Experimentally, the applied tension is closer to 80 kV than 57 kV that implies less turn in the cyclotron in order to pass the first RF gaps.

3

TECHNICAL DEVELOPMENTS

3.1 A cryogenic target for secondary ion beams

P. Dolégiéviez, Ph. Robillard, M. Ozille

A cryogenic system has been designed to make a thin target of solid hydrogen usable under vacuum, with a particle beam. This document describes the system developed and presents the results obtained with a 1 mm thick target with a diameter of 10 mm used with the first beam of SPIRAL facilities.

INTRODUCTION

The development of solid phase hydrogen targets is part of the research program with secondary ion beams [1]. The main requirements imposed for such targets are: low thickness, very fine windows, and uniform thickness and density.

Target systems have already been designed in various laboratories, particularly by directly condensing H_2 gas to make the target [2,3]. In the system developed, we opted for a transition to the liquid phase (16.2K / 23 kPa) before progressive solidification of the hydrogen (T< 13.9K) [4].

Liquid helium is used as a cold source at 4 K and the growth of the target is imposed by the temperature gradient in the metal frame supporting the target.

DESCRIPTION OF THE SYSTEM

Principle

The target is made using a metal frame to which mylar windows are glued. A stack of frames forms an H_2 target cell with an He cell on either side of the target.

During the target production phase, equivalent pressure is maintained on either side of the target windows. To do this, the pressure of a volume of helium gas matches the pressure variations of the hydrogen circuit during the phase transitions and up to the complete formation of the solid H_2 target (Figure 1). Once the target is formed, the helium gas is evacuated. The mechanical strength of the windows of the He circuit with respect to beam vacuum imposes the filling pressure, and hence the phase change temperature of the target gas.

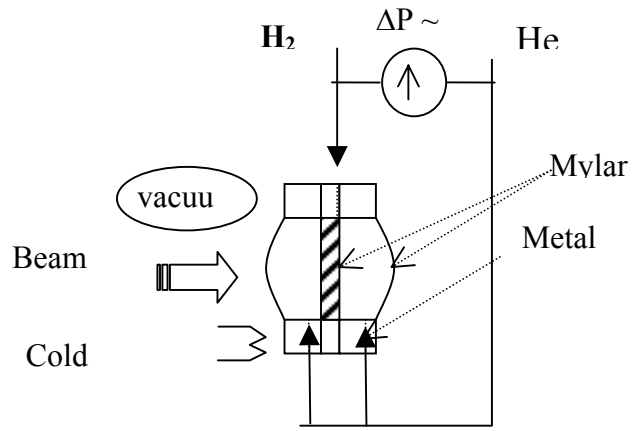

Figure.1 Shaping of the target

Cryogenic system

The cryogenic system consists of a cryostat with liquid helium circulation, of which the cold thimble (T = 4K) is mechanically coupled with the lower part of the target. This configuration helps to establish a temperature gradient aimed to make the solid grow towards the upper portion of the target. The gases enter through stainless steel capillaries (Φ 1-2 mm) welded at the bottom of the target for He and at the top for H_2. A thermalisation point is used from the cold thimble to reduce the power input by conduction of the capillaries at the top of the target. However, to prevent clogging, the H_2 circuits are kept at T>14 K during the target filling phase. This condition is essential to prevent the formation of bubbles caused by a lack of hydrogen feed during the formation of the solid.

The heat balance of the system gives a power received at the target of about 10 mW, 50% of it from thermal radiation (opening up the target to the beam axis). The heat transfer analysis reveals the possibility of obtaining the desired growth of the solid, by using brass (intermediate thermal conductivity) and by adopting a suitable geometry for the target frame (Figure 2). This solution offers a compromise between the cooling of the target and the maintenance of the hydrogen gas in the capillaries in the gas phase.

Figure 2 The target with the capillaries

Figure 3 Overall view of the device with 80 K shield

Calculations were made to determine the effect of the power deposited by the particle beam on the cryogenic target. With the beams used, the temperature elevation at the target remains negligible. The limit above which the triple point of H_2 is approached appears to lie around 10mW for a 4 mm diameter beam [5]

For the remainder of the system, a liquid nitrogen circuit ensures the thermalisation of the capillaries of the target at 80 K as well as the cooling of a shield to limit the radiation towards the device. The change in temperature in the system is monitored by silicon diodes. The overall vacuum system is supported by a stainless steel flange to vacuum standard DN 160 ISO-K (Figure 3).

Results

The results were obtained with a 1 mm thick target and 6 μm mylar windows. The observation of solid growth showed that as the temperature drops, the temperature gradient allows for the presence of the three H_2 phases in the target. The H_2 targets produced display no visible defect (Figure 4). The time required to produce the solid target, after placing the cryostat under vacuum, is about 3 hours and the system consumes ~1 l/h. of liquid helium to maintain the solid target at low temperature (depending the vacuum level).

The target was placed in the experiment vessel to intercept the beam during near a week (Ne 18 / P~20 μW on the target) and during all the experiment, the target temperature has stayed below 9K.

Figure 4 Hydrogen target : solid growth

REFERENCES

[1] W. Mittig and P. Roussel-Chomaz : Results and Techniques of Measurements with Invers Kinematics, Nuclear Physics (2001) A 693 495-513.
[2] P.E. Knowles, et al. : Nucl. Instr. and Meth (1996) A 368 604
[3] S. Ishimoto, et al. : A Windowless Solid Hydrogen Target, June 2000 KEK preprint (2000)-23 H
[4] P. Dolégiéviez, Ph. Robillard, Ph. Gallardo, M. Ozille, D. Heuze : Cryogenic system for a thin solid hydrogen target, November 29,(2000) Report Ganil A 00 01
[5] M. Ozille : Ganil report (2002)

3.2 EFFICIENCY AND PRODUCTION YIELD MEASUREMENTS OF RADIOACTIVE O, N AND F FOR THE SPIRAL FACILITY

S. Gibouin, ACC. Villari, JC. Angelique, O. Bajeat, F. Bocage, JM. Casadjian, S. Essbaa, G. Gaubert, Y. Huguet, A. Joinet, P. Jardin, S. Kandri, A. Khouaja, F. Landre-Pellemoine, C. Lau, N. Lescene, H. Lefort, R. Leroy, C. Marry, L.Maunoury, D. Nayak, JY. Pacquet, MG. Saint-Laurent, C. Stodel

Production efficiencies of radioactive oxygen and nitrogen beams for the SPIRAL target-source system, measured at GANIL on the SIRa test bench, are presented. From the overall efficiency of oxygen, the product between the efficiency of transformation of O into CO and the effusion of CO from the target to the ion source, was deduced. The production yield measurements of oxygen and nitrogen isotopes performed on the SIRa test bench and those of fluorine directly measured on the SPIRAL facility are presented.

1. INTRODUCTION

Based on isotope separation on-line (ISOL) [1], the SPIRAL facility [2] at GANIL delivers beams of radioactive isotopes. These isotopes are produced by fragmentation of a stable primary beam in the SPIRAL target, diffuse out of it and effuse up to an electron cyclotron resonance ion source (ECRIS), where they are ionised. After their extraction from the source, the radioactive isotopes are selected by a separator magnet before being injected into the cyclotron CIME [3] to get medium energy ions. The first radioactive beam ($^{18}Ne^{4+}$), corresponding to the commissioning of the SPIRAL facility, was sent to the experimental area at the end of September in 2001 [4]. The present target-source [5] system can supply radioactive beams of noble gases, with a dedicated target for He and another one for Ne, Ar and Kr. Furthermore, gaseous isotopes or molecules produced in the target could also be efficiently transported to the ion source, which would allow ionising and post-accelerating alternative radioactive beams.

In particular, oxygen and nitrogen radioactive beams are presently of great interest, mostly for astrophysics, e.g. $^{15}O(\alpha,\gamma)^{19}Ne$ [6] and direct reactions studies, e.g. $^{13}N(p,t)^{11}N$ [7]. The SPIRAL carbon target produces important amounts of oxygen and nitrogen molecules (CO, CO2, CN, etc.) allowing a fast transfer from the target to the ion source. This phenomenon is well known and was already used to produce radioactive beams at LISOL [8] and more recently at CRC, Louvain-la-Neuve [9]. For a more detailed review of ISOL oxygen beams, see reference [10]. Finally, the oxygen and nitrogen molecules are efficiently ionised in the ECRIS, which is the SPIRAL ion source [11]. Therefore, all ingredients necessary for an efficient production of these elements are present in the SPIRAL target-ion source system.

In this paper, we present the results of production efficiency and production yield measurements of radioactive O and N beams measured at the SIRa [12] test bench, and the production yield of radioactive F directly measured in the SPIRAL production cave. The expected production rates on the SPIRAL facility are also given.

2. EXPERIMENTAL SET-UP

The production efficiencies and production yields of radioactive oxygen and nitrogen beams have been measured on the SIRa [12] test bench at GANIL with the target-source system already developed for the production of radioactive neon, argon and krypton. The target, shown in Fig. 1, is made of a 1 μm graphite microstructure (POCO Graphite industries) in a conic shape with slices of 0.5 mm spaced by 0.8 mm, linked by an axis. It can be heated up to 2450 K by sending a current through its axis (the evaporation rate of carbon becomes important for the target above this temperature) to get a fast diffusion of the produced radioactive isotopes. The target is connected to a compact full permanent magnet ECR ion source (NANOGAN3 [13]).

The connection between the target container and the ion source is at room temperature. Therefore, for very reactive elements like oxygen, nitrogen and fluorine, the transport of the radioactive species is possible only if volatile molecules would be synthesized. The chemical nature of the target (carbon) plays an important role in this case.

The overall efficiency ξ of the production processes can be described, for example, for the reactive element O and for this target-source system, as follows :

$$\xi_O = \xi_{O\text{-}CO} \cdot \xi_{diff}(CO) \cdot \xi_{eff}(CO) \cdot \xi_{ion}(O/CO) \cdot \xi_{trans}(O) \quad (1)$$

The right hand terms of equation (1) respectively represent the transformation efficiency of O into CO, the diffusion efficiency of CO, the effusion efficiency of CO, the ionisation efficiency of O coming from CO and the transport efficiency of O. The product $\xi_{diff}(CO) \cdot \xi_{eff}(CO)$ is lifetime and temperature dependant, but this is not the case of the product $\xi_{ion}(O/CO) \cdot \xi_{trans}(O)$.

For the overall efficiency measurements, we simultaneously implanted secondary ^{14}O and ^{13}N beams, produced by projectile fragmentation using the SISSI device [14,15], in the target of SIRa. The implanted ^{14}O and ^{13}N were identified and quantified by Time-Of-Flight with a plastic detector placed just before the target. Non-ambiguous identification of ^{14}O and ^{13}N were provided at the end of the test bench, by the detection of the 2312.6 keV gamma ray for the first element and the 511 keV rays from β^+ annihilation for the second one, by using a germanium detector. The overall efficiency for each isotope is given by the ratio between their measured quantities at the end of the test bench and those implanted in the production target.
For the production yield measurements, we directly bombarded the SIRa production target with a ^{16}O beam of 95 A.MeV. The quantities of ^{14}O, ^{15}O and ^{13}N were measured, after selection by the separator magnet, at the end of the test bench.

3. EXPERIMENTAL RESULTS

3.1 Efficiency measurements

The different contributions to the overall efficiency of ^{14}O beam production for a target temperature of 2000 K was investigated by measuring the intensities of each molecular compound, as represented in Fig. 2. We assume that the ^{14}O implanted in the target was released under the molecular form CO (due to the enormous quantity of carbon atoms compared with others impurities). The other molecules were presumably created in the plasma of the ion source by a chemical reaction with mainly hydrogen, nitrogen, water, etc. The overall efficiency of ^{14}O found in all charge states and any molecular compounds was equal to 6.5(4) %.

The overall efficiency of ^{14}O beam production, as a function of the target temperature, was also investigated. These measurements are shown in Fig. 3. We can observe that around 2000 K a production plateau is reached. Therefore, one may conclude that for ^{14}O ($T_{1/2}$ = 70.6 s) the diffusion efficiency reached 100 % at this temperature. Concerning effusion, this is not the case, mainly because the transfer between target and ion source is cooled.
Moreover, we performed complementary off-line measurements on the ionisation efficiency of O coming from CO. In this study, a known quantity of stable $^{13}C^{16}O$ was injected through a alibrated valve. The quantity of ionised ^{16}O (including molecular forms) was measured at the end of the separator magnet. The ratio between these two quantities represents the ionisation efficiency of ^{16}O coming from $^{13}C^{16}O$, so-called $\xi ion(^{16}O/^{13}C^{16}O)$. The ionisation efficiency of ^{13}C coming from $^{13}C^{16}O$, so-called $\xi ion(^{13}C/^{13}C^{16}O)$, was also measured and found approximately similar. Therefore, we assumed that both ionisation efficiencies are equivalent, i.e.

$$\xi_{ion}(^{13}C/^{13}C^{16}O) = \xi_{ion}(^{16}O/^{13}C^{16}O) = \xi_{ion}(^{14}O/^{12}C^{14}O) \quad (2)$$

Considering a total beam transport efficiency of 53(5) % - also measured off-line using a ^{40}Ar calibrated leak - we obtained $\xi_{ion}(^{16}O/^{13}C^{16}O) = \xi_{ion}(^{14}O/^{12}C^{14}O)$ equal to 29(9) %. Finally, one can conclude that for ^{14}O ($T_{1/2}$ = 70.6s) at 2000 K, the product between the transformation efficiency of O into CO and the effusion efficiency of CO between target and ion source is:

$$\xi_{14O\text{-}12C14O} \cdot \xi_{eff}(CO) = 42\ (13)\ \%\quad (3)$$

Similarly, the overall efficiency for ionisation of ^{13}N was also measured at 2000 K. We obtained 0.67(5) % for $^{13}N^{1+}$, 0.047(8) % for $^{13}N^{3+}$, 0.048(5) % for $^{12}C^{13}N^+$ and 0.032(11) % for $^{13}N^{16}O^+$. In the case of nitrogen, the CN molecule is not an inert molecule at room temperature like CO. Therefore, the transport of radioactive nitrogen is less efficient.

3.2 Expected production rates on SPIRAL

The production yields of 14O, 15O and 13N were measured at the SIRa test bench impinging a limited intensity of 0.25 pμA of a 95 A.MeV 16O primary beam (corresponding to 380

W) directly on the carbon target, heated at about 2000 K. The average production rates obtained during 2 days of irradiation are presented in Table 1. From these results, we extrapolated the production rates for SPIRAL supposing a maximum beam power of 1500 W of a suitable primary beam (cf. Table 1). A 50 % transmission factor of the SPIRAL separator was assumed, provided that the correct adaptation of the beam to the injection of CIME imposes beam losses. It should be noted that the intensities obtained on-line are in perfect agreement with the estimations using the EPAX [16] model and the efficiencies measured in the preceding session.

^{18}F production yields were also directly measured on the SPIRAL facility by impinging 0.2 pμA of a 95 A.MeV 20Ne primary beam on the SPIRAL target. We obtained 2 x 10^5 p/s at the exit of the CIME cyclotron, corresponding to around 8 x 10^5 p/s just after the ion source. It is expected that with a 1500 W primary beam of ^{19}F, the final production rate of ^{18}F will be around 1 x 10^6 p/s.

In the framework of SPIRAL developments, the production efficiencies and production yields of radioactive O and N beams have been studied on the SIRa test bench. The overall efficiency measurements of oxygen and nitrogen have been presented, indicating that many molecules are created not only in the target zone but also in the plasma of the ion source. The efficiency of ^{14}O beam production as a function of the target temperature has been determined and its saturation was observed at 2000 K. Finally, the product between the efficiency of transformation of O into CO and the effusion of CO from the target to the ion source has been deduced. This mechanism is responsible for an efficient transport of oxygen from the target to the ion source plasma.

Production yield measurements of oxygen, nitrogen and fluorine isotopes have been presented. The expected production yields for SPIRAL have been extrapolated. The yield measurements are in perfect agreement with theoretical calculations using EPAX model folded by the efficiencies measured in this paper.

4. CONCLUSION

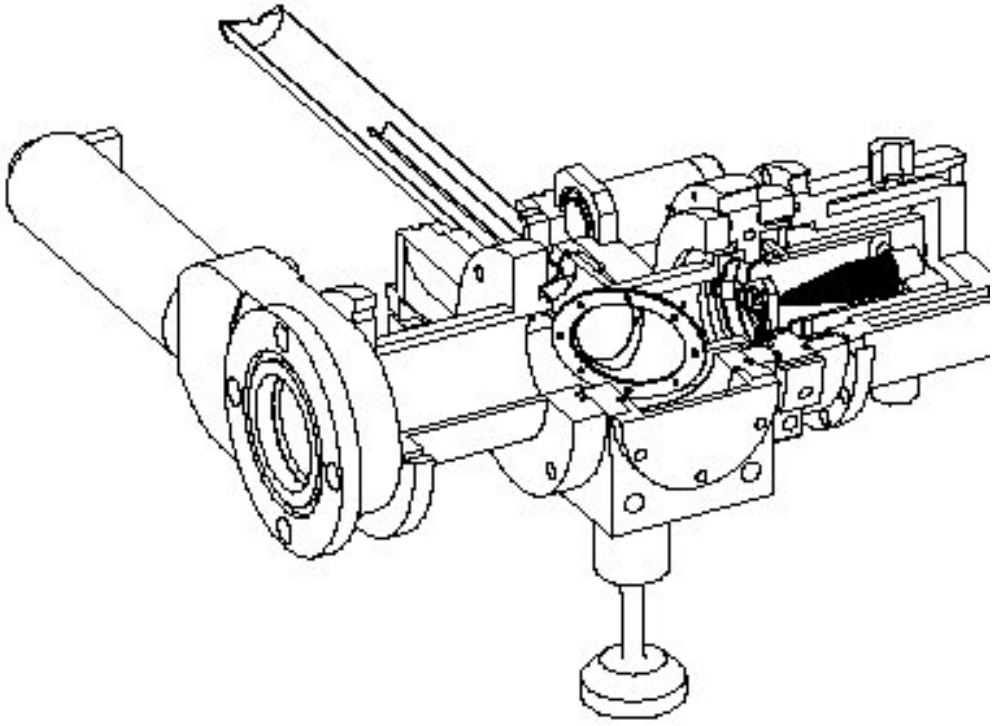

(1) Technical drawing of the Target-Part of the SPIRAL Target-Source production system. The target used for the production of radioactive Ne, Ar and Kr beams is shown.

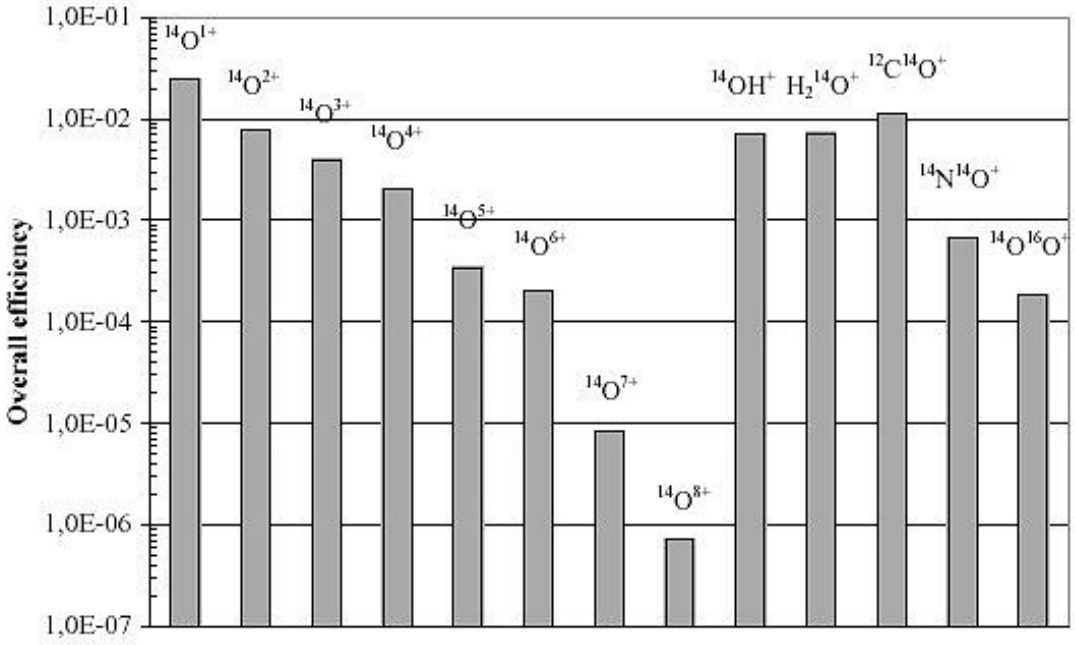

(2) Different contributions to the overall efficiency of ^{14}O measured on the SIRa test bench, for a target temperature of 2000 K. The intensity of the $^{12}C^{14}O^{16}O^{+}$ molecule is not represented because its quantity is negligible compared with $^{12}C^{14}O^{+}$.

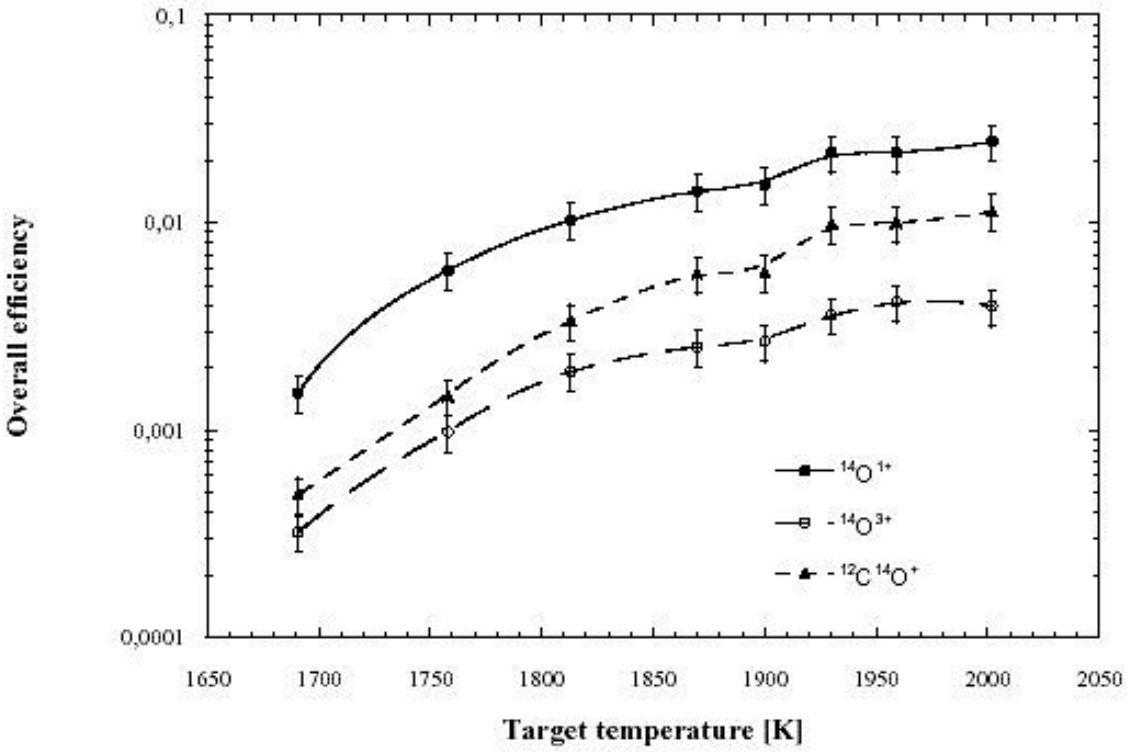

(3) Overall efficiency of $^{14}O^{1+}$, $^{14}O^{3+}$ and $^{12}C^{14}O^{1+}$ on the SIRa test bench as a function of the target temperature. A line is drawn to guide the eye.

Ion	Primary beam used on SIRa	Mean production rate measured on SIRa and normalised by 380W of primary beam	Primary beam on SPIRAL	Expected production yield at the entrance of CIME
$^{14}O^{1+}$	$^{16}O^{8+}$ 95 A.MeV	7.2 (1.4) 10^6 p/s	$^{16}O^{8+}$ 95 A.MeV	1.4 (0.3) 10^7 p/s
$^{14}O^{2+}$		2.2 (0.4) 10^6 p/s		4.3 (0.9) 10^6 p/s
$^{14}O^{3-4+}$		8.4 (1.7) 10^5 p/s		1.7 (0.3) 10^6 p/s
$^{14}O^{5-6+}$		2.2 (0.4) 10^5 p/s		4.4 (0.9) 10^5 p/s
$^{15}O^{1+}$		2.3 (0.5) 10^8 p/s		4.6 (0.9) 10^8 p/s
$^{15}O^{2+}$		7.0 (1.4) 10^7 p/s		1.4 (0.3) 10^8 p/s
$^{15}O^{3-4+}$		2.7 (0.5) 10^7 p/s		5.4 (1.1) 10^7 p/s
$^{15}O^{5-6+}$		7.2 (1.4) 10^6 p/s		1.4 (0.3) 10^7 p/s
$^{13}N^{1+}$		1.4 (0.3) 10^7 p/s	$^{14}N^{7+}$ 95 A.MeV	5.0 (1.0) 10^7 p/s
$^{13}N^{2+}$		2.5 (0.5) 10^6 p/s		9.0 (1.8) 10^6 p/s
$^{13}N^{3+}$		4.0 (0.8) 10^5 p/s		1.5 (0.3) 10^6 p/s
$^{13}N^{4-5+}$		5 (2) 10^4 p/s		2 (1) 10^5 p/s

(4) Production yield measurements on the SIRa test bench and production yields extrapolated for SPIRAL when choosing the best primary beam. The $^{15}O^{5-6+}$ production yield on SIRa has been extrapolated by using the efficiency measurement of $^{14}O^{5-6+}$.

REFERENCES

[1] O. Kofoed-Hansen, K.O. Nielson, K. Danske Vidensk. Selk, Medd. 26, N° 7, 1951.
[2] A.C.C. Villari, Nucl. Phys. A693 (2001) 465.
[3] M. Duval, M.P. Bourgarel, F. Ripouteau, IEEE Trans. Magn. 32 (1996) 2194.
[4] A.C.C. Villari et al., this conference.
[5] F. Landré-Pellemoine, PhD thesis, GANIL T 01 03, 2001.
[6] J.M. D'Auria, Nucl. Phys. A701 (2002) 625c
[7] J.M. Oliveira Jr. et al., Phys. Rev. Lett. 84 (2000) 4056.
[8] N. Severijns et al., Phys. Rev. Lett. 63 (1989) 1050.
[9] M. Loiselet et al., CAARI 16, AIP Conf. Proc. n. 576 ed. by J.L. Duggan and I.L. Morgan, (2000) 269.
[10] U. Köster, in Eur. Phys. J. A, in press.
[11] A.C.C. Villari et al., Nuclear Instruments and Methods in Physics Research B126 (1997) 35.
[12] P. Bricault, Proceedings of the 13th International Conference on Cyclotrons and Applications, Vancouver, (1992) edited by G. Dutto and M.K. Craddock, World Scientific, p. 725.
[13] L. Maunoury et al., Proceedings of the 18th International Workshop on ECR Ion Sources, College Station, Texas USA, edited by P. May and E. Ramirez, (1997) p.138.
[14] A. Joubert et al., IEEE Particle Accelerator Conference, San Francisco, USA, Vol. 1 (1991) 594.
[15] N. Lecesne et al., Nuclear Instruments and Methods in Physics Research B126 (1997) 141.
[16] K. Sümmerer and B. Blank, Phys. Rev. C, Vol.61, N°3 (2000) 034607.

METALLIC ION BEAM DEVELOPMENTS

C. Barué , C. Canet, M. Dupuis, J.L. Flambard, G. Gaubert, Y. Huguet, P. Jardin, N. Lecesne, P. Lehérissier, F. Lemagnen, R. Leroy, J.Y. Pacquet, F. Pellemoine-Landré.

Abstract

An overview of the production methods mainly used at GANIL is presented in this report. Experimental observations and recent results about germanium beam production at high intensity are detailed.

1 INTRODUCTION

Intense ion beams from gaseous elements are easily and routinely produced by ECR ion sources. It is not so easy for metallic elements for several reasons :

• *evaporation of the sample :*

most of the time, the metallic element to ionize is under solid form. It must be evaporated into the source plasma. Although high intensities can be produced with the oven method (80 µA Ca^{11+}) [1], it becomes more difficult for low vapor pressure elements. Nickel is a good example : increasing the production of nickel by increasing the oven temperature (typically above 1500°C) would prematurely damage the oven.

⇒ *the method must produce enough metallic atoms injected into the plasma in order to reach the intensity required for the experiment.*

• *ionization efficiency :*

since most of the metallic atoms or ions condense on the cold plasma chamber walls, the evaporation rate has to be higher compared to gas operation : the metallic consumption is typically 10 times higher for a given intensity level. This high consumption is not compatible with the use of rare and expensive isotopes, mostly requested by physicists. The ionization efficiency has to be as high as possible.

⇒ *the ionization efficiency has to be maximized in order to produce the required intensity during the total experiment time while consuming no more than the given amount of rare isotopes.*

• *beam stability :*

The chemical reactivity of metallic atoms condensed on the plasma chamber walls influences the source stability. For example, strong chemical getter effects have been observed when using a mixing gaz, leading to uncontrollable intensity flushes (see section 4).

⇒ *the stability must be good or very good depending on the experiments. At least, it must stable enough to tune the accelerator.*

2 CONFIGURATION

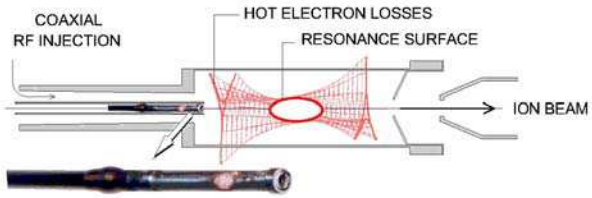

Figure 1 : *Source configuration. The axial RF injection and the biased tube are represented. An axial access is available through the biased tube. The micro-oven developed at GANIL is represented on this drawing.*

Two ECR ion sources are used for the primary beam production at the GANIL facility : the source "ECR4" [2] developed at GANIL, and an improved version "ECR4M" [3] characterized by a stronger magnetic confinement. Both sources work at 14 GHz. The first one is placed on a high voltage plate-form to extract the beam up to 100 kV, and the second one has a 25 kV mono-gap extraction system.

Due to the coaxial RF injection, only one axial access to the plasma is available. This point is of importance for metallic ion beam production : the sample (oven, electrode, etc...) is just located in front of the hot plasma losses and therefore, extra heating of the sample by the plasma itself can not be neglected. Using an oven for example, the source tuning could significantly influence the evaporation rate.

All the results presented in this report have been obtained with this configuration.

3 PRODUCTION METHODS

Only the production methods mainly used at GANIL are presented in this section : the "oven" and the "MIVOC" methods. A complete overview of the methods tested and used at GANIL can be found in reference [4]. An updated list of available beams can be consulted on our web page [5].

3.1 The oven method

This method is well suited to elements having a vapor pressure between 10^{-3} and 10^{-1} mbar for a temperature lower than 1500°C and higher than 300°C. This functioning area is represented in Fig. 2 .

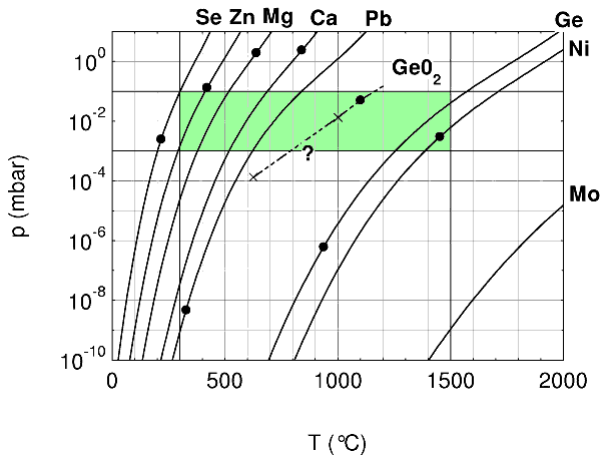

Figure 2 : *Vapor pressure of some elements versus temperature. The melting point is represented by a black dot.*

Above 1500°C the components of the oven (heating wire and crucible) are quickly damaged, decreasing drastically the life time of the oven. As an example, this is the main reason why nickel beam intensity is limited with this technique : high vapor pressure is reached at too high temperatures (see Fig. 2).

Below 300°C the evaporation is dominated by plasma heating, due to the location on axis of the oven. As an example, we were not able to control selenium production in this configuration : selenium immediately evaporates as soon as the plasma is ignited. For selenium, we overcame the difficulty by placing a small disk just in front of the oven (see picture) : it was possible to control a stable intensity of 1.5 µA $^{80}Se^{9+}$ (natural : 50%) during 4 hours and with a consumption around 0.6 mg/h. To increase further the intensity and to eliminate the risk of sur-evaporation, a "low temperature oven" has to be developed [6].

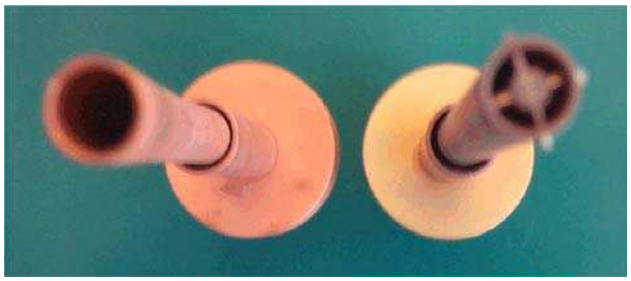

On the left : the coaxial tube , on the right : modified coaxial tube for selenium production (October 2000).

The use of chemical elements melting before reaching the working vapor pressure could be troublesome. The phase change happens within a fraction of a second and is very violent : the liquid instantaneously migrates toward the cold parts of the oven. This has been observed on-line elsewhere using a camera during operation. This violent migration could obstruct the mouth of the oven or eject the metal outside the oven.

It happens sometimes with lead, for no well-known reasons, that the oven empties very quickly. Melting the sample before operation with the oven in vertical position could help to overcome this difficulty.

Oxides can be preferred to pure metals because they melt at higher temperature (GeO_2 for example). Moreover, they sometimes have higher vapor pressure helping evaporation : molybdenum beam has been produced using its oxide form (MoO_3) whereas it would not be possible with pure molybdenum.

Most of the metallic ion beams are produced with the oven technique at GANIL : Mg, Ca, Pb, Sn, etc...[4].

Our micro-oven has been successfully used for the production of calcium 48. The ^{48}Ca beam has been accelerated up to 60 MeV/u with an intensity of 0.13 pµA on target (740 W beam power). Description and results can be found in reference [1].

3.2 The MIVOC method

This method is now routinely used at GANIL for the production of nickel beams at high intensity : a maximum intensity of 70 eµA has been obtained for natural nickel (68% : ^{58}Ni) on charge state 9+ and at 20 kV extraction voltage. The total extracted current from the source was 5 emA.

At this maximum intensity, we observed repetitive sparks, about one spark every second, in the source extraction leading to periodic beam lost during a fraction of a second. Running the source in argon at the same intensity level (5 emA) showed no instability at all. Therefore, these sparks are probably due to the presence of nickelocene molecules in the extraction area. This spark problem must be studied and solved.

The main limitation of the MIVOC method is the high total extracted beam intensity. Thus it seems impossible to further increase the nickel intensity.

More information can be found in references [7][8].

4 RECENT DEVELOPMENTS

4.1 Germanium

This development was initiated by a request for a ^{76}Ge beam at high intensity. First results have been presented at the last ICIS conference at Oakland [1]. They are detailed in this report.

One of the difficulty is the strong chemical reactivity of germanium. We choose the oxide form GeO_2 to reduce the chemical attack of the sensitive parts of the oven (heating wire). The use of pure metal quickly destroys the first turn of the heating wire in direct view of the evaporation. Moreover, the evaporation of GeO_2 form requires a lower temperature (see Fig. 1), and therefore strongly diminishes chemical attack by germanium.

Several tries have been done to find the good procedure and source parameters. The use of helium as mixing gaz improved the stability and the reproducibility of the results.

An intensity of 8.5 eμA $^{74}Ge^{12+}$ natural (36%) has been produced for 48 h. The temperature of the oven had to be progressively increased from 950°C up to 1100°C to maintain this intensity (see Fig. 4). The consumption was 1 mg/h, i.e. 0.25 mg/h ^{74}Ge. The total ionization efficiency was around 5% without transport correction.

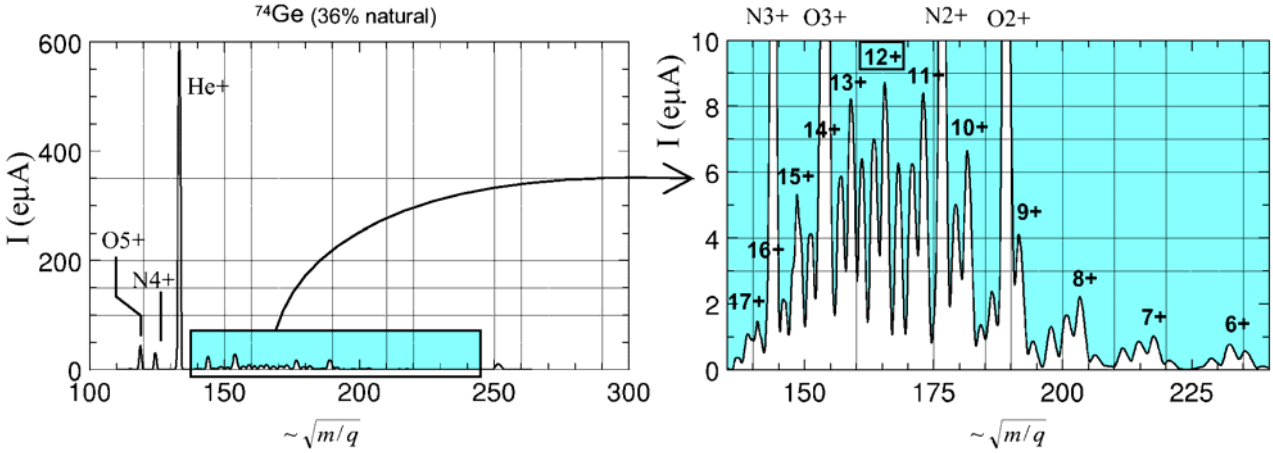

Figure 3 : *Natural germanium spectrum (^{74}Ge : 36%, ^{72}Ge : 28%, ^{70}Ge : 21%) optimized on $^{74}Ge^{12+}$ for stability : an intensity of 8.5 eμA has been maintained for 48 h. Extraction voltage : 71 kV, total extracted current : 1.4 emA, RF power : 115 W, source : ECR4, mixing gaz : He, oven position : +7 mm inside the plasma chamber, electrical power of the oven : 15 W (~1000°C), date : March 13th, 2002.*

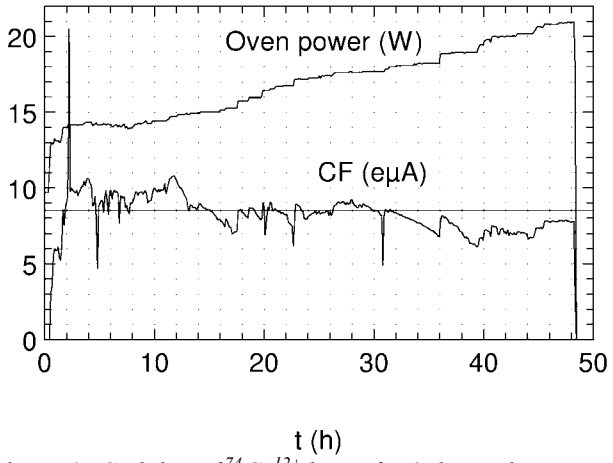

Figure 4 : *Stability of $^{74}Ge^{12+}$ beam for 2 days. The temperature oven was increased from 950°C up to 1100°C to maintain the beam intensity.*

Some interesting behaviours have been observed during and after germanium tests.

• *Chemical getter effect :*

When producing germanium at higher intensity we have observed very strong chemical getter effect although inert mixing gaz (He) was used : the high intensity fall down by one order of magnitude within a few minutes. A spectrum made during this regime has shown that almost no helium was present. By decreasing the evaporation rate of germanium it was possible to come back to a stable situation. No solution has been found to overcome this getter effect at very high intensity.

• *Walls coating effect :*

After the metallic tests we run the source with argon to see the source performance after the germanium contamination. It was a surprise to produce 200 eμA of Ar^{9+} and more over with a good stability ! It has never been obtained before so easily. We concluded that it was probably a wall coating effect with GeO_2.

• *Recycling germanium :*

Since source performance were good in argon after the germanium tests, it was decided to keep the same plasma chamber for the next scheduled beams. It was a big mistake ! First beam for physics (Ne) has been produced without problem. The next planed beam was ^{36}S using $^{36}SF_6$. It was impossible to reach the expected intensity of 20 eμA for $^{36}S^{10+}$: 10 eμA could be obtained with difficulty. Looking at the spectrum (see Fig. 5), we observed that an important amount of natural germanium (12 eμA of $^{74}Ge^{12+}$!) was present in the plasma. Consequently, this presence of germanium degraded so much the charge states distribution of suffer that it was impossible to produce the required intensity on the high charge state 10+. The plasma chamber had to be replaced by a new one. Then, after outgazing the source, it was easy to get 20 eμA of $^{36}S^{10+}$ and we could give the beam back to the physicists. We explained the presence of germanium in the plasma by a chemical reaction between germanium condensed on the wall and fluorine, producing GeF_2 molecules. The compound GeF_2 having a high vapour pressure, it can be re-evaporated into the plasma.

Although this unexpected experiment reduced the beam time for physics, we were satisfied to learn that it is possible to recover germanium condensed on the plasma chamber walls by using SF_6 and moreover with a high intensity : 12 eμA of $^{74}Ge^{12+}$, i.e. about 30 eμA Ge^{12+} with 100% isotopic enrichment ! How long ? recycling efficiency ? remain open questions. This recycling possibility is of interest for very expensive isotopes like ^{76}Ge and in view of the important amount of germanium remaining in the plasma chamber (95%, i.e. 5% ionization

efficiency). It has to be further investigated in terms of stability and efficiency.

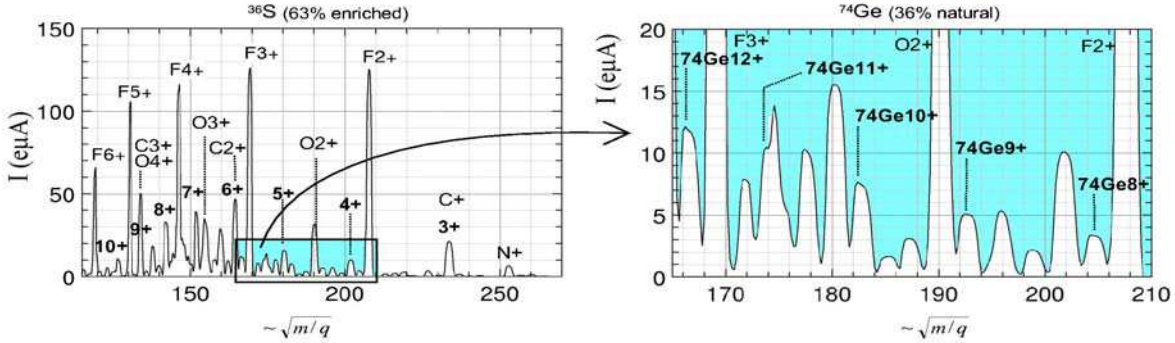

Figure 5 : *Recycling of germanium by using SF_6. RF power : 384 W, extraction voltage : 72 kV, total extracted current : 1.5 emA, source : ECR4, no mixing gaz, date : October 17th 2001.*

4.2 Oven

Two different developments are under way :

• *bigger oven* :

At present, the micro-oven used for metallic ions production is small. The inner diameter of the crucible is 1.5 mm and the length is 30 mm, i.e. about 0.045 cm^3. It allows a maximum load of 70 mg for calcium or 500 mg for lead. With the new oven being developed the crucible volume has been increased to 0.141 cm^3. The maximum load capacity will range from 220 mg up to 1.6 g.

It will increase the functioning time and will facilitate the introduction of samples inside the container.

The evaporation of elements with this oven is being tested off-line.

• *high temperature oven :*

The goal is to increase the temperature up to 2000°C and consequently extend the list of available metallic ions (U for example).

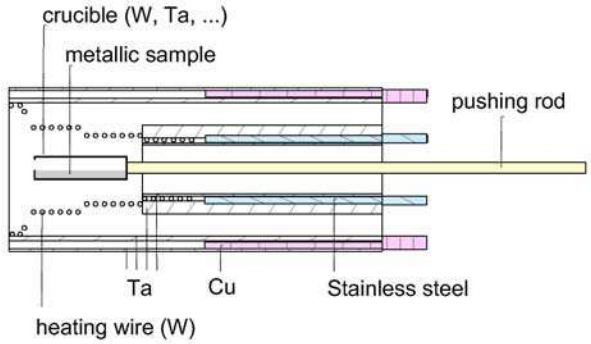

Figure 4 : *Sketch of the high temperature oven.*

The background idea was to remove all Al_2O_3 parts of the oven which are sensitive to very high temperatures. The melting point of Al_2O_3 depends on its quality.

The high temperature oven avoids electrical contact between the heating wire and the crucible. Therefore, crucibles made of very refractory material (W, Ta) can be used and high temperatures can be reached. A temperature of 1800°C has been measured for a relatively low electrical power of 350 W. A temperature higher than 1700°C has been maintained for 50 hours.

Evaporation tests with vanadium were successful (vapor pressure is 10^{-2} mbar at about 1850°C).

5 FURTHER IN METALLIC ION BEAM PRODUCTION ?

The ionization efficiency remains low for metallic ion production : it rarely exceeds 20%. Most of the time, the ionization efficiency is lower than 10%.

It has no importance if the samples are available in abundance, and if it exists a method produce high enough vapor pressure. Nevertheless, for rare and expensive isotopes, the ionization efficiencies have to be improved. Since so many years the metallic ion production methods have been investigated, it seems to show a limitation in terms of ionization efficiency.

The nice results obtained at the ISN Grenoble on the 1+ –> N+ method [9], i.e. 50% ionization efficiency, could be used for the benefit of metallic production. Depending on the existence of a metallic ion source producing mono-charged ions with 100% ionization efficiency, we could inject this 1+ beam into a N+ source, to get an overall ionization efficiency of 50% ! For example : 100 µA of Ni+ will be enough to reproduce the best result of the MIVOC method. The efficiency of 50% for such 1+ intensity has to be confirmed.

6 NEWS FROM GANIL

• *SPIRAL* :

The safety authorisations to start the SPIRAL installation finally arrived. The first radioactive beam of $^{18}Ne^{4+}$ (1.67 s) has been produced on September 21st 2001 : a 300 W primary beam of ^{20}Ne was sent into the target-source assembly to produce 3 10^6 pps of $^{18}Ne^{4+}$

Until now, $^{8}He^{+}$, $^{8}He^{2+}$, $^{72-77}Kr^{11+}$ have been produced by the SPIRAL facility with a primary beam power up to 1.4 kW.

7 CONCLUSION

Metallic ion production raises new and interesting problems. The chemistry and the ion source configuration are important factors for metallic ion beam production. The development of a new metallic beam requires numerous tries before answering to the feasibility questions : performance, reliability, consumption and stability.

Efforts are still being made to improve the intensity and extend the list of available metallic beams. However, it remains many open questions. The ionization efficiencies are still low and have to be improved : new methods must be investigated.

References

[1] P. Lehérissier et al., 9th ICIS conference, September 2001. To be published in Rev. Sci. Instrum.

[2] P. Sortais et al., Rev. Sci. Instrum. 61, p. 228 (1990).

[3] R. Leroy et al., 12th Int. workshop on ECR ion sources, Riken, 1995, p. 57 (1995).

[4] L. Bex et al., Rev. Sci. Instrum. 69, p. 792 (1998).

[5] http://www.ganil.fr/user/experiments

[6] K. Tinschert et al. Rev. Sci. Instrum. 69, p. 709 (1998).

[7] News from GANIL, n°67, p. 11, mars 2001. http://www.ganil.fr/research/sp/ng.html

[8] C. Barué et al., PHIBI workshop, Catania, Sept. 2000.

[9] N. Chauvin et al., internal report, ISN99.112 (1999).


4
THI

4.1 OPTHI Project

A. Savalle

I Goals

The objective was to enable the operation (tuning, supervision, security) of THI beams for use with SISSI and SPIRAL targets. The goals are more precisely defined in [1].
The project had to define and realize :

- The necessary conditions for surety and security of equipments
- The means to improve the stability
- The instrumentation needed to measure the beam characteristics
- The algorithm of the programmable logic controllers and of the software related to the THI security modes
- In addition, the project was extended to the possibility to send a THI beam directly to the experimental areas.

II Realization

II.1 Surety :

The first way of producing exotic nuclei at GANIL uses fragmentation in the target of SISSI. The THI beam, passing through this target, loses a part of its energy and is defocused. It may be lost upon different elements, comprised between SISSI and the first dipole of the Alpha spectrometer.
Collimators have been disposed to protect some equipments (like emittance slits) from this beam. However, some elements, disposed upstream the first collimator, may be activated. Two actions were undertaken :
- A radiological zone, including the beam line between SISSI and the collimators, where access is strictly limited, was defined.
- The intensity modulator, which was disposed upstream the first collimator, has been removed and reinstalled downstream. This equipment is, thus, protected from the primary beam slowed in the SISSI target [2], and its activity is lower.

II.2 Security of equipments :

A programmable logic controller is used to control the tuning and beam supervision, so that no unacceptable beam losses can occur.
In order to improve the security of the equipments situated downstream SISSI, against the primary beam, these equipments (collimators, emittance slits, intensity modulator) are now controlled with this programmable logic controller.
Similarly, SPIRAL has been taken into account (beam loss detectors in line L4, differential current transformer L3-L4 protect the equipments when the beam is sent to the SPIRAL target). [3].
The related software has been improved.

II.3 Stability [4]

The means and the way to stabilize the accelerators have been revisited. Two general principles were applied :

- The feedback loops are no more designed to make the beam central phase constant but to stabilize the equipment (ex. the R.F. voltage of the cyclotrons).
- The sensitivity of the measurement, versus the equipment to stabilize, is maximized.

Thus :
- The magnetic field level are no more used to maintain the beam central phase constant, but are periodically checked by MNR measurement.
- the R.F. voltage of the injector cyclotron is no more used to stabilize the beam central phase at the entrance of SSC1 (with a very low sensitivity), but is stabilized by measurement of the energy. Note that this measurement is made by a beam position probe in the low energy spectrometer, situated in front of the energy slits. By this way, the transmission of the beam line L1 can be stabilized, while it was not necessarily true with the former feed-back loop.
- similarly, a feed-back loop involving the R.F. voltage of the SSC1 cyclotron and a beam position probe in the “chapeau de gendarme” spectrometer has been checked.

II.4 THI MODES [5]

3 THI «modes » have been defined :

- injector mode : the beam is stopped in the beam line from the injector to SSC1 : the beam power is limited due to the low energy
- tuning mode : the beam intensity is limited. Interceptive diagnostics may be inserted. This mode is to be used for tuning.
- Supervision mode : the beam intensity is not limited. Interceptive diagnostics may not be inserted

Initially, in tuning mode, the beam intensity was limited with a pepper pot. It was shown that, due to space charge forces without pepper pot, the transmission in SSC2 cyclotron and the beam characteristics were changed when removing the pepper pot. Consequently, a part of the tuning had to be made in the supervision mode, without any possibility to insert some diagnostics (like beam profile monitors).

The THI tuning mode has been modified, so that : The intensity is no more limited with a pepper pot, but with the beam chopper , at a rate of 1/6 for a 2 kW beam, 1/16 for a 6 kW beam.

However, it is still possible to change the beam chopping rate when the pepper pot is in.

Associated with this modification of the tuning mode, it was necessary to enable the insertion of the beam profile monitors, with the beam intensity limited by the chopper only.

II.5 New beam chopping rates [6]

The beam profile monitors at GANIL are secondary emission grids. In the beam line L3 (from SSC2 to SISSI or SPIRAL), these diagnostics may be inserted with a chopping rate lower than 1/100.

However, the energy deposited at SSC1 energy (beam line L2), is much higher, so that the necessary beam chopping rate may be as high as 1/1000.

This intensity reduction is obtained by this way :

- from 1/1 to 1/128 the beam pulse duration is unchanged (T_{on} = 950 μs) and the beam is stopped for an increasing duration, from T_{off} = 950 μs (1/2) to T_{off} = 127*950 μs = 120 ms (1/1000).
- When beam chopping rates higher than 1/128 are necessary, the beam pulse duration, equal to 950 μs at 1/128, T_{on} decreases to 120 μs at 1/1024.

To realize these new rates, the electronics of the chopper as well as the program of the programmable logic controller have been changed.

The insertion of the beam profile monitors at a high peak intensity, and, thus, the THI « modes » described in (II.4) are now available.

II.6 Measurement of the longitudinal emittance - « deltat » probes

The THI beam tests revealed that to understand the high intensity beam dynamics, the knowledge of the longitudinal emittance was essential.

Two non interceptive « delta t » probes have been installed, at the output of SSC1 and at the entrance of SSC2, to enable the measurement of the beam phase extension. The aim is to facilitate the tuning of SSC1 and of the rebuncher R2.

These probes are micro-channel plates, collecting electrons or ions from ionization of residual gas. At the entrance of SSC2, the probe may be used simultaneously to visualize the horizontal and the vertical profile [7].

This probes, as well as those which were installed previously in the beam line L3, have been connected to the GANIL command-control.

Consequently, they may be used in three modes [8] :

- visualization of the beam phase extension ($\Delta\phi$)
- longitudinal emittance reconstitution by measurement of $\Delta\phi$ versus beam energy (using energy slits)
- supervision : as these probes are non interceptive, they may be used to warn the operators if the phase extension is increasing

II.7 Extension to the experimental areas

At high intensity, the accelerators and the beam lines are protected from beam losses with :

- beam loss detectors : graphite rings are disposed throughout the accelerators and the lines to measure beam losses
- « differential current transformers »: the beam intensity is measured by current transformers. The transmission through the accelerators and the beam lines is calculated. Depending on the beam power, the transmission must remain better than a given percentage.

When an unacceptable beam loss is detected, a security system is triggered which stops the beam , then reduces the beam power (the programmable logic controller imposes the tuning mode, see II.4).

The extension of THI to the experimental areas has required the installation of new beam loss detectors in the beam lines, as well as a completion of the electronics system using the differential current transformers.
THI may be used in three ways : SISSI, SPIRAL, and experimental areas. The use of THI is taken into account to valid or inhibit some beam loss detectors or differential current transformers.

III Conclusion

The routine operation of THI began at the end of 2001, and was pursued in 2002, with :

- several accelerations of $^{13}C^{6+}$, of beam power from 1 kW to 1.4 kW, for use with the SPIRAL target-source (production of ^{8}He and acceleration with CIME)
- The first THI beams used in LISE / LISE 2000 :

Ion	Energy (MEV/U)	Beam power (kW)
^{86}Kr	58	0.66
^{48}Ca	60	0.55
^{78} Kr	68	0.65

[1] Cahier des charges fonctionnel DIR/P/OPTHI-017
[2] DIR/P/OPTHI-023 « tache Opération - Modulateur»
[3] DIR/P/OPTHI-026 Cahier des charges fonctionnel du système INTERLOCK THI
[4] DIR/P/OPTHI-024 « tache Opération - Asservissements»
[5] DIR/P/OPTHI-025 « Nouveaux modes THI»
[6] DIR/P/OPTHI-022 « Modification de la réalisation des rythmes hacheur »
[7] DIR/P/OPTHI-029 « Compte-rendu EM du 2/12/01 »
[8] DIR/P/OPTHI-006 « Cahier des charges de l'application Deltat »

4.2 THI6K project (6 kW beam acceleration)

M-H. Moscatello

1. Goals

Initially, this project aimed at proposing different means of accelerating a 6 kW beam, limited to 2.10^{13} pps, in safety, security, and reliability operational conditions.
After the first studies, it appeared that it was more logical to extend the project goals to some equipment realisation and to high intensity beam effective acceleration.

2. New radial probe in the injector

The injector cyclotron radial probe has been redesigned (Figs 2.1 and 2.2), in order to stand a higher thermal power, 200W for a 1MeV/A beam [1]. Moreover, some "high" and "low" probes have been added, in order to measure the vertical movement of the beam in C01.

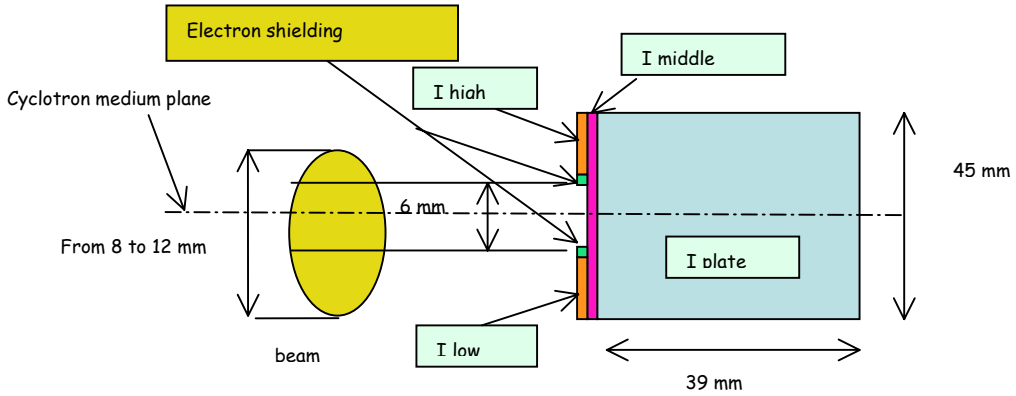

Fig. 2.1. : principle of C01 radial probe

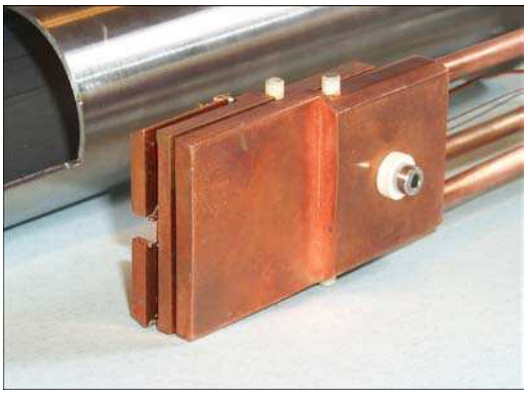

Fig. 2.2 : photography of the new radial probe

3. Beam dynamics in C01 with the "round beam" model

Several machine studies were performed in C01, in order to understand the large transverse emittance at the cyclotron exit and (try to) create a "round beam", with a phase extension decreasing with the radius; this phenomenon would lead to a smaller energy dispersion at the accelerator exit.
Up to now, this "round beam" phenomenon has been observed only in PSI, with a very high intensity beam, in which this effect creates itself along the acceleration, thanks to the space charge forces. It has also been demonstrated (theoretically and numerically) that such a phenomenon could take place even without space charge forces, under some specific correlations at the cyclotron injection [2].

During these studies in C01, several technical problems were encountered, and needed to be solved in order to progress in the studies:

2.3.1 Search for the origin of the"50 Hz" problem and elimination of it

2.3.2 Restarting of the phase extension probe at C01 exit

- Elimination of the buncher delay line problems
- Search for the apparent isochronism problem, corrected by a variation of the central isochronism coil current

Moreover, a systematic vertical beam oscillation has been seen with the new radial probe, it remains unexplained up to now.

With all these solved problems and improvements, the next “round beam” machine studies should give better results; one must also choose a better adapted beam, for which the space charge are maximised in C01.
The addition of a rebuncher at the injector entrance would permit to increase the injected beam intensity in C01, and even without space charge effects, it would give the possibility of creating the necessary energy dispersion to create the round beam conditions (this would be also interesting for CIME cyclotron)

4. Increase of the SSC2 dee voltage

The SSC2 dee voltage had been operated at 170 kV (@13.45 MHz), for many years, as there had been no need for higher values. When ion beam powers were increased up to several kW, space charge effects appeared in SSC2 [3], mainly due to turn overlap. Thus, an increase in the dee voltage was needed and a detailed study of the possible performances of the SSC cavities was done [4], which confirmed that they could reach voltages as high as 250 kV, at high frequency, 13.45 MHz (fig.4.1). Furthermore, the operating diagram of the 100 kW amplifiers (Fig 4.2) was obtained in order to estimate the required RF power, with the available measurement points.

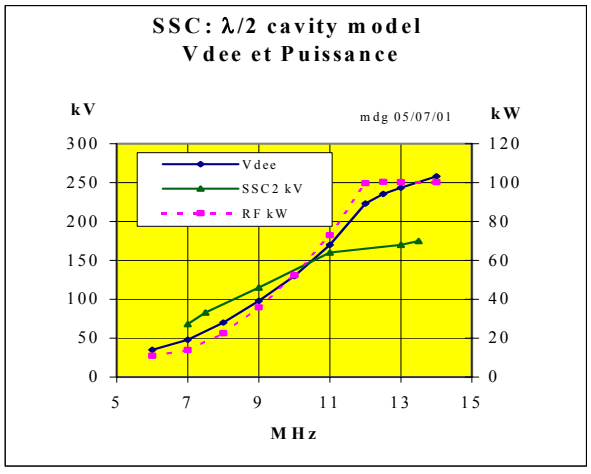

Fig. 4.1 : Dee voltage law including the power limitations

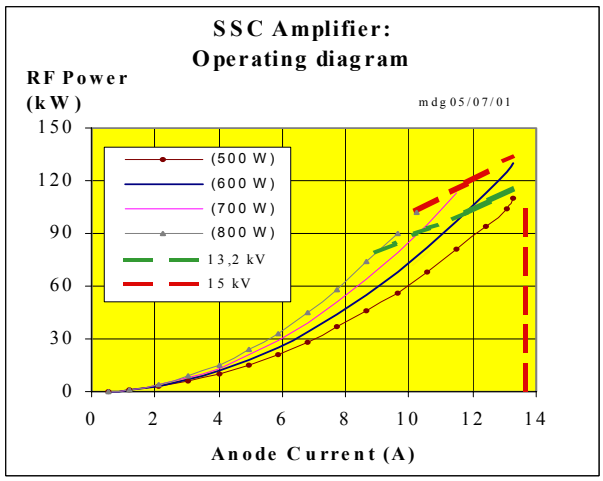

Fig. 4.2. Operating diagram of the 100 kW amplifiers

After a new tuning of the amplifiers on a 600 Ohm operating point, 210 kV were obtained on both cavities without any problem, which allowed to accelerate a 5 kW beam. Some tests were also performed at 230 kV during a few hours, value corresponding to the accelerating needed voltage for a 6 kW beam. Moreover, some X-ray measurements confirmed that RF voltage calibration were not very precise, and that the North cavity had a real voltage 10-15% higher that the South one (which proofs that it can already be operated around 230-240 kV in CW operation).

5. Acceleration of a 5 kW ^{36}Ar beam

The Argon beam profile presented on figure 5.1 has been registered in the extraction region of CSS2, and corresponds to the last accelerated turns, with a RF voltage of 200 kV. On the figure, both curves correspond to 2 different tunings of the rebuncher R2 (placed upstream of SSC2 to optimise the injected beam phase).
With this tuning, the overall transmission of the cyclotron is equal to 97%, (the 3% losses are located on the electrostatic deflector pre-septum) and the ejected beam intensity equal to 26 μA, corresponding to a thermal power of 5 kW for a 95 MeV/A Argon beam.

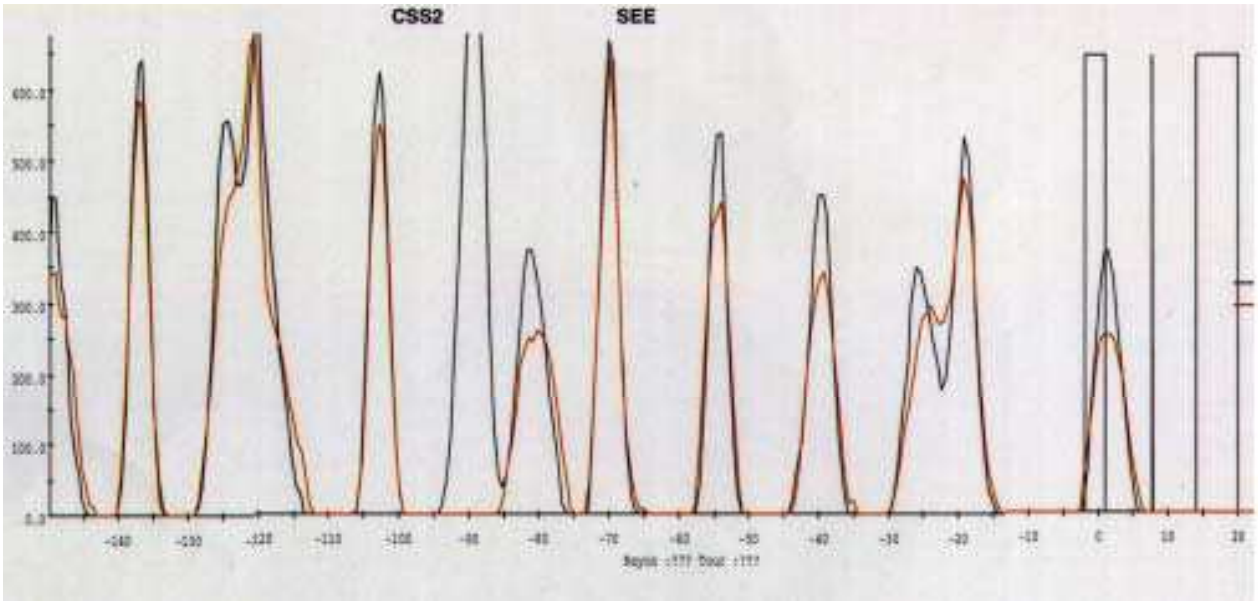

Fig.5.1. Turn pattern of a 5 kW Argon beam in the extraction region of SSC2 (black curve)

6. SSC2 electrostatic deflector modifications

The pre-septum has been redesigned to reduce beam losses (thickness=1mm instead of 2mm), and the thin plate material has been changed from Copper to Tungsten, in order to reduce in particular the long term activation of this equipment. The cooling circuits have been redesigned (maximum beam losses will be of the order of 300 Watts, but everything is designed for supporting 600 Watts) as well as the whole mechanical supporting structure [5]. The copper septum thickness had to be reduced at the entrance of the deflector (from 1 mm to 0.5 mm), while the thickness at the exit remains the same: 3mm. The scheme of this new system is presented in figure 6.1.This equipment will be installed in the accelerator during summer 2003

7. Conclusion

The studies and realisations described above have improved the understanding in the operation of several equipment, and should allow the acceleration of 6 kW beams, with beam losses and operation conditions compatible with the present operation mode.

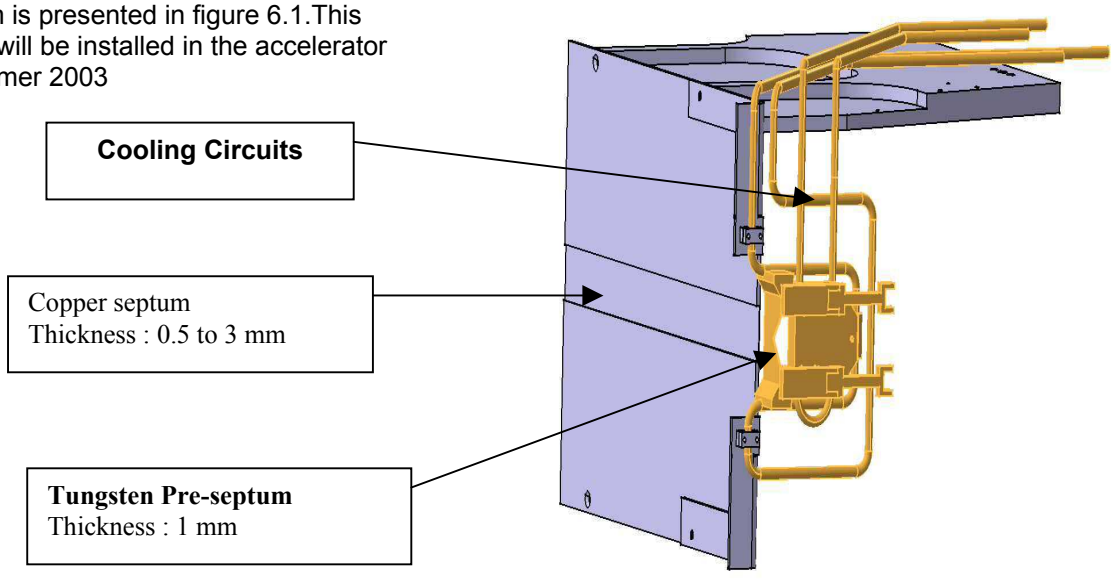

Fig.6.1. Scheme of the new pre-septum

8. References

1: P. Anger,“ Tête de sonde radiale de l’injecteur C01”, Internal reports 2001-2002
2 : P.Bertrand, C.Ricaud , Specific cyclotron correlations under space charge effects in the case of a spherical beam, Proceedings of the 16th International Conference on Cyclotrons and their Applications, East Lansing, USA, 2001, p.379-382
3 : E. Baron et al, “High intensity heavy ion beams for exotic nuclei production at Ganil”, Proceedings of the 16th International Conference on Cyclotrons and their Applications, East Lansing, USA, 2001
4 : M. Di Giacomo,“ Etude préliminaire sur les limites des systèmes HF des CSS afin d’en augmenter l’intensité crête”, Internal report, DIR/P/THI6K-05,2001
5: F.Pellemoine, “ Etude thermique et mécanique d’un nouveau septum pour CSS2 dans le cadre du projet THI6K”, Internal report, THI/SST/DIA/000/TH/NT/A/0188/A

5

NEW EXPERIMENTAL FACILITIES

5.1 IRRSUD

F. Loyer

1. GOALS

IRRSUD is an irradiation facility using the low energy beams (0.3 to 1 MeV/n) coming from the injectors.

IRRSUD is sponsorised by GARI (Groupe d'Applications de la Recherche avec les Ions) whose objectives are to develop the applied and industrial research with ions.

Among the numerous experiments which will be carried on, we may note :

- nanotechnology research : it is the use of the matter structure modifications by the ion impact
- study of the mattre ageing under irradiation. The main case is the study of the fission fragment effect simulated by the low energy ions.

The IRRSUD beam line can be used as a test bench for the beam coming from the injector.

2. MAIN CARACTERISTICS

IRRSUD consists of :

- A beam line which transports and adapts the beam from one of the injectors to the irradiation bench. The injector providing the beam is the one which is not on line with the accelerator. According cases, this injector is C01 or C02.
- An irradiation bench
- A cave where the beam line and the irradiation bench are installed
- A building to welcome the physicists who prepare and manage the experiments

2.1 Beam Line Caracteristics

The main beam line caracteristics are :

- keeping the initial caracteristics of the beam injected into the accelerator (CSS1)
- insuring the focus of the beam, either in the scanning magnet plan (5 mm radius spot), or on the irradiation target (3 mm radius spot)
- providing instrumentation to tune (position, profile, intensity,...) and survey the beam
- allowing the emmittance tuning
- insuring a scanning of 50 mm in both planes on the target
- leaving room to insert complementary equipements later

The main components of the line are (see drawings above) :

- dipoles to guide beam from the injector output towards the IRRSUD line
- 1 steerer for each plane to correct the beam trajectory (horizontal one is included inside the dipoles)
- 4 quadrupoles to focus the beam
- 4 profiles probes
- 1 Faraday cup
- 1 intensity transformer
- 1 beam stopper before the irradiation bench
- vacuum system to reach 10^{-7} mbar

2.2 Irradiation Bench Characteristics

The irradiation chamber is similar to those existing in the high and medium energy lines of GANIL. This allows to use directly all the equipment already available.
However, the range of the IRRSUD ions generally does not allows to place in a window to disconnect the vacuum of the beam line and the atmosphere of the irradiated samples. A sample holder, movable by 30 cm, allows irradiation of series of samples without breaking the chamber vacuum. This plate can be cooled by room temperature water or by a refrigerated fluid. Liquid nitrogen cryostats are available for low temperature irradiation. They can be easily put in and removed without warming the samples.
Four independent slits are used to cut the scanned beam for tuning the irradiated area. The intensity of the beam is continuously monitored by measuring the ion current on the peripheral region of the irradiation spot.

2.3 Cave Description

The beam line and the irradiation bench are installed inside a cave whose access is not controlled by the security system because the ion beam energy is under the coulomb barrier.
However, because of the radiation coming from CSS1 through the biologic protections, this cave is classified as a "zone surveillée" (dose rate < 7.5 μSv/h) whose access is reserved to authorized people.
A small crane allows to carry equipments.
The walls of the injector caves have been moved to create this new cave. (see the scheme of the facility below)

2.4 Building Description

A new building has been built to put at physicists' disposal the facility they need to prepare and manage the experiments. It consists of :

- a room to control the acquisition and the equipments
- an office where to work and to discuss
- a laboratory where to prepare the experiments

Moreover, a corridor insures the access to C01 and CSS1.
At least, in order to intervene on the electrostatic components of the accelerator, a laboratory has been added besides the IRRSUD building.
The below scheme describes succinctly this building.

3. Results of the beam line tests

The beam line IRRSUD was checked with a C02 beam ($^{84}Kr^{15+}$ at 0.66 MeV.A). The transmission was around 96%.
The beam line, from C02 to IRRSUD, is supposed to be doubly achromatic. A slight change of the quadrupoles gradients was found necessary. This is made by an automatic beam tuning software.
The beam widths, measured in both planes with the profile monitor ISFST12, were +/- 8 mm, compared to +/- 6 mm expected. This corresponds to the normal uncertainty upon the be am characteristics at the output of the cyclotron. A manual tuning of the two last quadrupoles (ISQ13 and ISQ14) enables easily to get the nominal characteristics.
The beam line requirements are satisfied.

4. Project Milestones

- **Winter 1999-2000** : modifications of the injectors environment (walls, beam security, radiologic protection, deviation dipoles) in order to insert the IRRSUD beam line further.
- **Winter 2000-2001** : construction of the beam line
- **Spring 2002** : construction of the building
- **22th may 2002** : authorization by the safety authority (DGRSN) to use IRRSUD with beam
- **June 2002** : beam line commissioning
- **October 2002** : first experiment

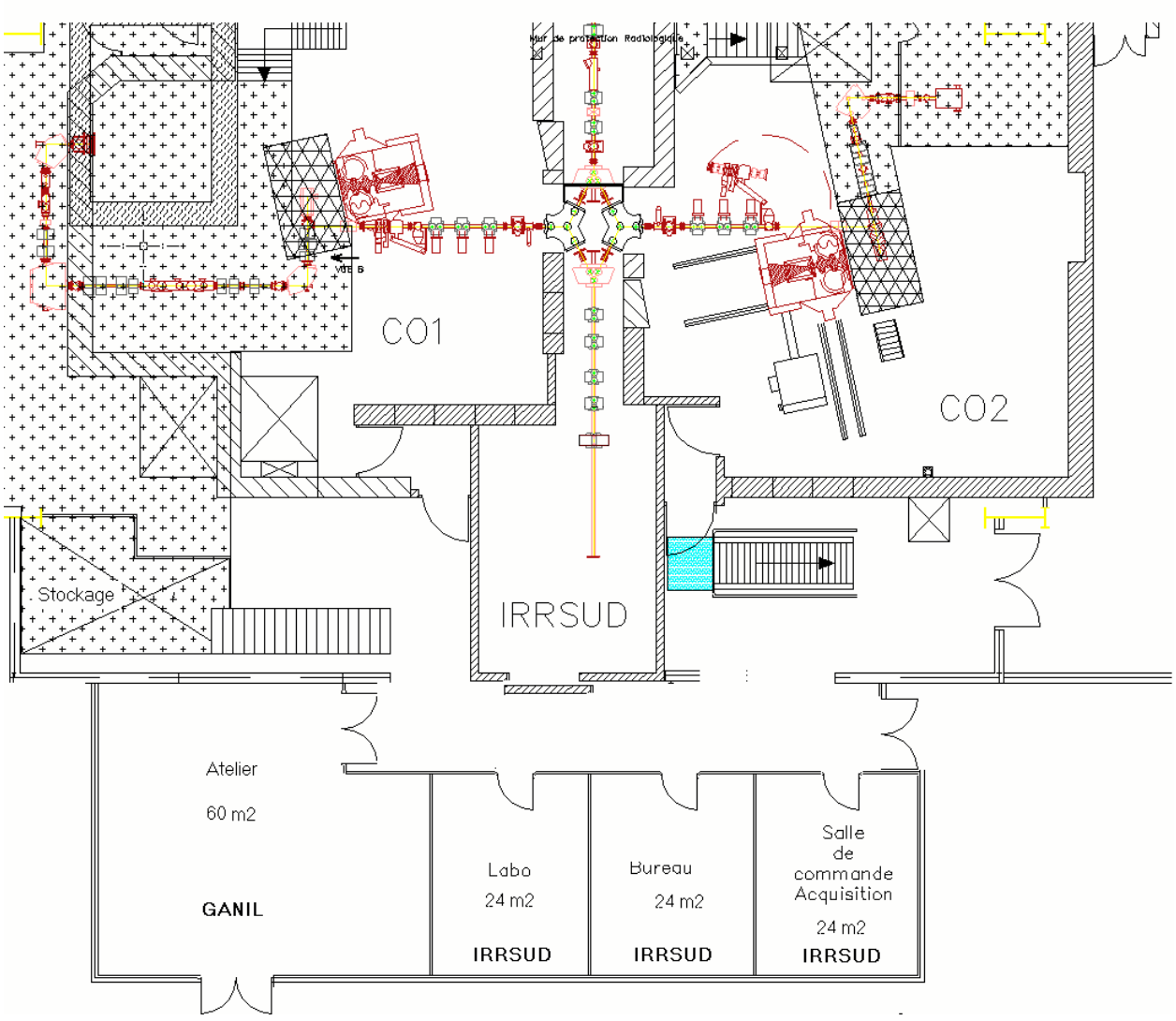

IRRSUD Implantation Scheme

IRRSUD beam line
(without the irradiation bench)

IRRSUD Building

5.2. LIRAT PROJECT

A. Peghaire

1. GENERAL PRESENTATION

1.1 Objectives

With the arrival of radioactive ion beams (SPIRAL) we found of great interest to open a new facility devoted to the study and to the use of very low energy radioactive beams, between 10 to 30 KeV/A. The principle is to use directly the very low energy beam extracted from the ion-source of SPIRAL, without any acceleration.

The aim of such a beam line was discussed in various GANIL Scientific Committees (December 1998, June 2000 and December 2001). The scientific program with a very low energy may cover a large variety of research fields as :

- static properties (mass, spin, parity, quadrupole moment …) and nuclear decays of nuclei
- study of fundamental interactions (test of standard model, test of CPT, …)
- study of solid state and atomic physics

1.2 Global project

The global project is presented in fig. 1. We plan to focus the radioactive beam outgoing the SPIRAL target-ion source to an unemployed room of approximately 200 m^2 located on the north basement of the machine area.

In red we present the full LIRAT project, while we have put in green the possible future extensions, in particular the connections with the new SPIRAL II project. The line is calculated to admit three experiments at the same time.

1.3 First step project

Unfortunately, the funding of the project has been delayed, so we have decided to build the first part of the line, this one allowing to realize an experiment proposed by the LPC of Caen. This experiment is at present in test and will be ready to operate at the beginning of 2004.

This first part of the line is presented in Fig 2. From the ion source the line uses a part of the SPIRAL low energy beam line, up to the identification device beam line. A switching magnet is inserted just in front of the identification device. This will allow to use a same beam in the cyclotron CIME, in the identification device or in LIRAT facility. The beam will be focused by the use of 5 Q-poles and 4 steerers (labeled LTQxx and LTDCxxVE or HO in the figure). The beam tuning will be controlled by 4 beam profilers (labeled LTPRxx).

2. STATE OF PROGRESS IN MAY 2003

Today, at the fall of May 2003, quite all the mechanical parts of the line (supporting elements, beam tubes, magnetic components) are mounted. All the main elements are ordered. All the connections to the rest of the GANIL commands will be installed before the end of this year. The aim is to drive a stable beam in this line before the fall of this year, and why not, to have also a radioactive beam test.

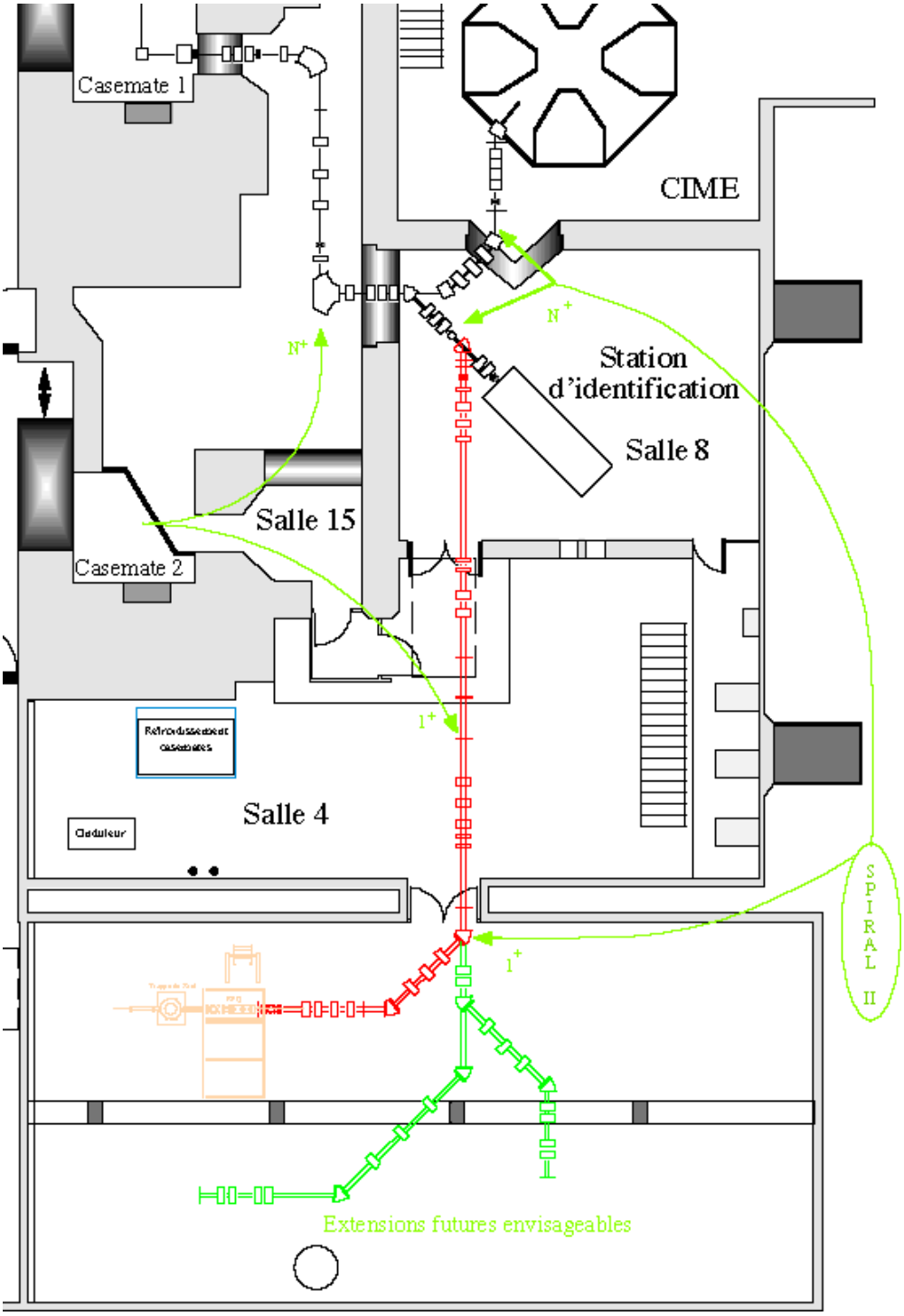

Fig 1. Full LIRAT beam line (in red) with the possible extensions (in green)

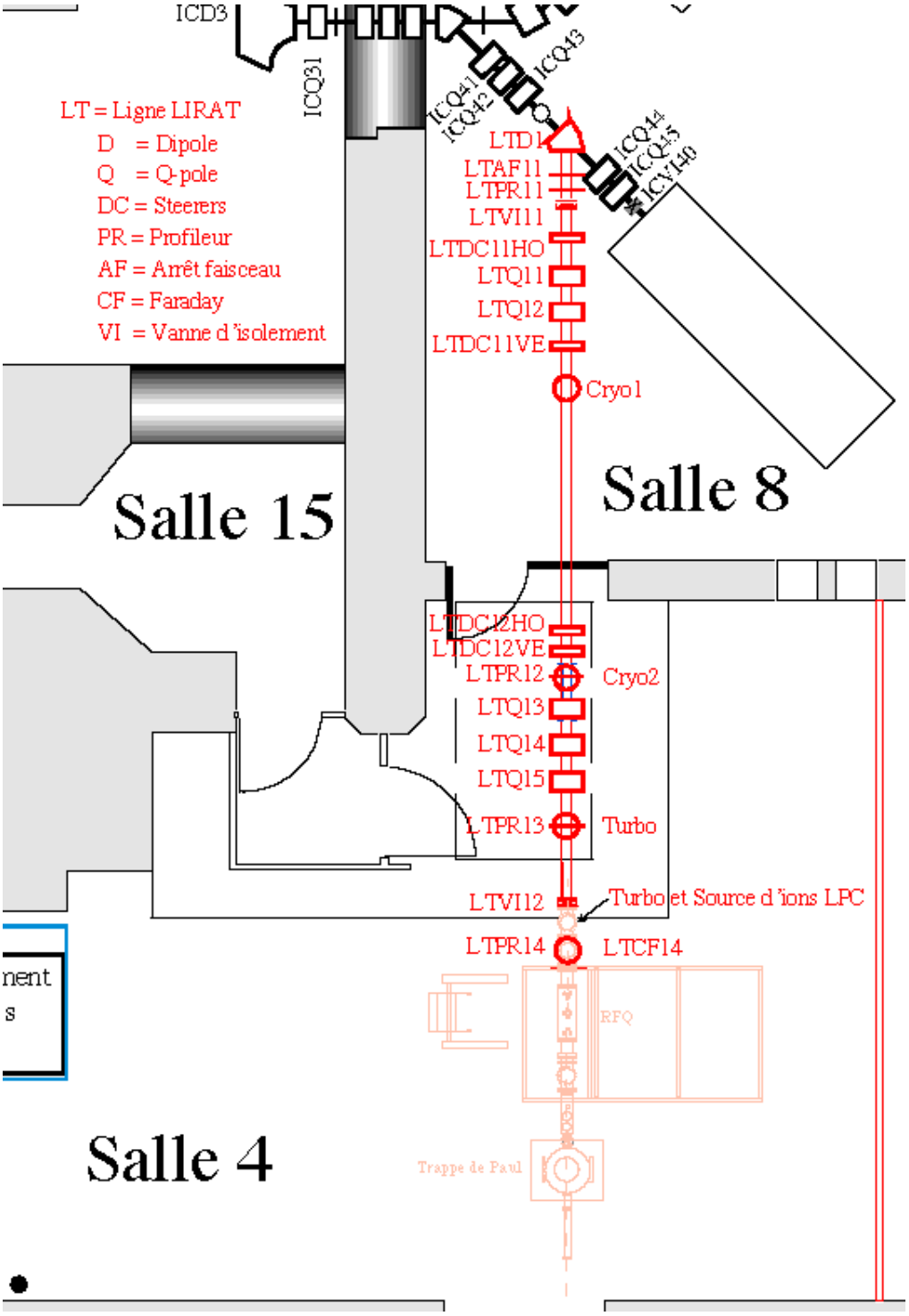

Fig 2. First part of LIRAT as it will be at the end of 2003.

Appendix #1

EXPERIMENTS CONDUCTED IN NUCLEAR PHYSICS

YEAR 2001

Date	Exp #	Duration *hours*	Title	spokesperson	Beam	Energy *A.Mev*
9 March	E287b	189,25	High resolution in-beam gamma-spectroscopy study of light neutron-rich nuclei	Azaiez	^{36}S	77.5
30 March	Sira	72		Saint-Laurent	^{20}Ne	95
2 April	E372	311,75	Multifragmentation and asymmetric nuclear matter in the fermi energy region	Borderie	^{124}Xe ^{136}Xe	45 45
19 April	E373	145	Excitation function of fusion-like heavy residues produced in collisions of very heavy systems	Frankland	^{129}Xe	27
25 April	E374	180,5	Experimental determination of universal fluctuations in central heavy-ion collisions at intermediate energy domain	Chbihi	^{129}Xe ^{129}Xe	27 35
10 June	E364	35,5	Mass measurements close to the neutron drip-line	Savajols	^{36}S	50
12 June	E379	155,5	Determination of the ground-state spins and moments of ^{43}S and ^{43}Cl	Neyens	^{48}Ca	60
19 June	E364	156,5	Mass measurements close to the neutron drip-line	Savajols	^{48}Ca	60
25 June	E377	262	Beta decay studies of neutron-rich S and P isotopes	Grévy	^{48}Ca	60
20 July	E334	184,5	Intruder ^{2}S 1/2 mixing in ^{12}Be	Orr	^{18}O	63
31 Aug.	E378	163	Multi-particle correlations and the structure of heavy He isotopes	Marques	^{13}C	60
6 Sept.	T2	91,5	Test	Freer	^{13}C	60
10 Sept.	T3	17,5	Test	Bouffard	^{13}C	60
12 Sept.	E378	177	Multi-particle correlations and the structure of heavy He isotopes	Marques	^{18}O	63
21 Sept.	Tspir	151	ECS Test - Identification - Stable beam Tunning	Test Spiral	^{20}Ne	95
27 Sept.	E400S	147	Spectroscopy of ^{19}Na from resonant elastic scattering	de Olivera	^{20}Ne	95
5 Oct.	E312c	195,5	Spectroscopic studies of proton-rich nuclei in the vicinity of ^{45}Fe and ^{48}Ni	Blank	^{58}Ni	75
7 Oct.	T4	64	Test D6	Blank	^{58}Ni	75
10 Oct.	E381	184,5	Study of the ground state and the first 2^+ and 3^+ state of the ^{22}O nucleus through elastic and inelastic proton scattering	Khan	^{58}Ni ^{36}S	75 77
9 Nov.	E405s	84	Study of ^{8}He + p elastic scattering at 16 A.MeV	Pollacco	^{13}C	75
13 Nov.	E396	61	Tests of the VAMOS spectrometer	Savajols	^{13}C	75
19 Nov.	E405s	184	Study of ^{8}He + p elastic scattering at 16 A.MeV	Pollacco	^{8}He	16.3
27 Nov.	E350as	46	Isobaric analogue states of ^{7}He and ^{9}He	Mittig	^{8}He	16.3
8 Dec.	E243b	232	Isomer and beta spectroscopy close to ^{78}Ni	Pfutzner	^{86}Kr	58

EXPERIMENTS CONDUCTED IN NUCLEAR PHYSICS
YEAR 2002

Date	Exp #	Duration *hours*	Title	spokesperson	Beam	Energy *A.Mev*
16 March	E383	86	Spectroscopy of neutron-deficient Po isotopes : First tests of recoil decay tagging studies with VAMOS	Becker	^{36}Ar	4.9
25 March	E392	179	Search for new neutron-rich nuclei with Z>10	Penionzhkevich	^{48}Ca	60
4 April	E408S	203	Competition between octupole and multi-particle excitations in Po-212 and At-213	Walker	^{8}He	3.5
13 April	E350a	28	Isobaric analogue states of ^{7}He and ^{9}He	Mittig	^{8}He	3.5
17 April	E339b	378	Formation and study of super-heavy nuclei via inverse kinematics reactions	Peters	^{208}Pb	5
23 May	E368a	157	Search for isomers in the N=Z nuclei ^{74}Rb, ^{68}Se and in the T_Z = -1/2 nucleus ^{71}Kr	Becker	^{78}Kr	68.5
31 May	E404S	167	Identification of gamma-ray in nuclei around ^{130}Sm : probing the maximally deforme light rare earth region	Nolan	^{82}Kr ^{76}Kr	4.6 4.6
17 June	E344aS	284	Shape coexistence near the N=Z line and collective properties of Kr isotopes investigated by low-energy Coulomb excitation of radioactive ion beams	Korten	^{82}Kr ^{76}Kr ^{74}Kr	From 2.6 to 4.6
2 July	E376	160	Mass measurement of exotic nuclei around the N=Z ^{84}Mo	Auger	^{58}Ni	4.3
9 July	E350aS	177	Isobaric analogue states of ^{7}He and ^{9}He	Mittig	^{16}O ^{8}He	3.9 3.9
15 July		28	Test	VAMOS	^{8}He	3.9
19 July	E281	143	The study of ^{6}He + ^{6}He cluster states in ^{12}Be	Freer	^{12}C ^{8}He	13 13
25 July	T9	20	Test SIRA	Saint-Laurent	^{8}He	13
29 Aug.	E403S	295	Role of weakly bound neutrons on fusion around the Coulomb barrier	Navin	^{18}O ^{6}He ^{8}He	From 2.9 to 5
6 Sept.	E283c	19	Coulomb excitation of ^{70}Ni and ^{66}Fe	Sorlin	^{13}C	75
10 Sept.	E418	27	Mass measurements close to the neutron drip-line	Savajols	^{13}C	75
18 Sept.	E283c	281	Coulomb excitation of ^{70}Ni and ^{66}Fe	sorlin	^{76}Ge	59
2 Oct.	T10	103	Test LISE 2000	Georgiev	^{76}Ge	59
5 Oct	T11	49.5	Test VAMOS	Pollaco	^{76}Ge	59
7 Oct.	E398	107	High-precision measurements of the decay of ^{21}Mg and ^{25}Si and its mirrors	Thomas	^{36}Ar	95
8 Nov.	T9	51	Test SIRA	Saint-Laurent	^{36}Ar	95
9 Nov.	T10	5.5	Test LISE 2000	Georgiev	^{36}Ar	95
11 Nov	E422S	257	Study of 4-neutron system using the d(^{8}He, ^{6}Li) reaction	Beaumel	^{12}C ^{8}He	15.4 15.4
21 Nov.	E378S	129	Multi-particle correlations and the structure of heavy He isotopes	Marques	^{12}C ^{8}He	15.4 15.4
30 Nov.	E415	160	Search for multineutrons and correlations in the breakup of ^{14}Be	Marques	^{18}O	63
10 Dec.	E384	154	Magnetic moment measurements of neutron-rich N=35 9/2+ isomers	Daugas	^{64}Ni	55
17 Dec.	T15	16	Test VAMOS	Savajols	^{64}Ni	6.9
19 Dec.	T14	35	Test INDRA	Morjean	^{64}Ni	6.9

EXPERIMENTS CONDUCTED IN SWIFT ION PHYSICS

YEAR 2001

Date	Exp #	Duration *hours*	Title	spokesperson	Beam	Energy *A.Mev*
9 March	P566	23	Etude des dommages cellulaires induits par des ions lourds : effets précoces	Testard	^{36}Ar	95
10 March	P549	16	Radiolyse des macromolécules biologiques par les ions lourds de TEL . 180 keV/um. Modélisation des effets biologiques de la réaction ^{10}B(n,a) ^{7}Li.	Charlier	^{36}Ar	95
11 March	P98-2	12		Levalois	^{36}Ar	95
12 March	P559	46	Radiolyse pulsée à TEL élevés avec les ions lourds. Réactivité dans les traces des radicaux libres de l'eau	Baldacchino	^{36}Ar	95
25 March	P523	8,5	Effets des ions lourds sur les régulations neuro-immunitaires	Marquette	^{20}Ne	95
5 May	P562	24	Détermination de l'Efficacité Biologique Relative (EBR) des ions ^{12}C : étude de différents critères et tests pertinents pour des applications en radioprotection et radiothérapie	Guelette	^{12}C	95
6 May	P543	16	Synthèse d'agrégats bimétaliques par radiolyse à haut TEL	Remita	^{12}C	95
9 May	P550	16	Ion track grafting study of different monomers on to CTA, PP Arel PUDF	Mazzei	^{208}Pb	29
11 May	P488	26	Défauts colonnaires et matière de vortex dans les supraconducteurs	Kes	^{208}Pb	29
12 May	P567	8	Création de défauts colonnaires dans les oxydes supraconducteurs	Soret	^{208}Pb	29
12 May	P554	20	Columnar defects in perovskite superconductors, an easy path for ozygen diffusion ?	Kes	^{208}Pb	29
30 Nov.	P566	20	Etude des dommages cellulaires induits par des ions lourds : effets précoces	Testard-Terleth	^{36}Ar	95
1 Dec.	P572	10,5	Radiolyse des macromolécules biologiques par les ions lourds de TEL . 180 keV/um. Modélisation des effets biologiques de la réaction ^{10}B(n,a) ^{7}Li.	Charlier	^{36}Ar	95

EXPERIMENTS CONDUCTED IN SWIFT ION PHYSICS
YEAR 2002

Date	Exp #	Duration *hours*	Title	Spokesperson	Beam	Energy *A.Mev*
23 March	P598	32	Radiolyse des macromolécules biologiques par les ions lourds de TEL . 180 keV/um. Modélisation des effets biologiques de la réaction $^{10}B(n,a)\ ^{7}Li$. 1 - Les protéines		^{36}Ar	95
	P608		Irradiation de cellules humaines par les ions à TEL élevé : corrélation trace physique/trace biologique, implications de certaines lésions précoces dans l'instabilité chromosomique retardée			
	P558		Signal transduction after high LET irradiation of human cells			
15 April	P562	21	Détermination de l'Efficacité Biologique Relative (EBR) des ions ^{12}C : Etude de différents critères et tests pertinents pour des applications en radioprotection et radiothérapie	Gueulette	^{13}C	75
3 May	P531	20	Cooling and heating of ions in crystals	Assman	^{208}Pb	5
5 May	P503	34	Distribution de vitesse des atomes éjectés par l'impact d'un ion lourd rapide	Bouffard	^{208}Pb	5
6 May	P506	44	Desorption of nanoclusters from nanodispersed targets of metals by swift heavy ions (^{208}Pb, E = 300 MeV - 6 GeV) in extremely hith energy regime of electronic stopping ((dE/dx)e=50-100keV/nm)	Baranov	^{208}Pb	5
10 June	P496	12	Local observation of defect reactions in solids	Wichert	^{76}Kr	4.6
11 June	P606	21	Effet du dépôt d'énergie par des ions lourds dans des dispositifs semi-conducteurs	D'Hose	^{78}Kr	68.5
113 June	P571	88.5	Interference effects in electron emission from H^2 by 95 MeV/u Ar^{18+}	Stolterfoht	^{78}Kr	68.5
27 July	P562	23.5	Détermination de l'Efficacité Biologique Relative (EBR) des ions ^{12}C : Etude de différents critères et tests pertinents pour des applications en radioprotection et radiothérapie	Gueulette	^{13}C	75
29 July	P569	64	Towards a better understanding of the processes of conversion of the energy deposited in the electronic system into atomic displacements	Dunlop	^{208}Pb	29
1 Aug.	P611	16	Vortex correlations in highly anisotropic superconductors	Kes	^{208}Pb	29
1 Aug.	P607	8	Dynamique des vortex dans des supraconducteurs à hautes température critique en présence de différentes configurations de défauts colonnaires	Ruyter	^{208}Pb	29
2 Aug.	P593	12	Irradiation of ion track templates for spin magneto electronic nanostructures	Hjort	^{208}Pb	29
28 Aug.	P593	37.5	Study of heavy ion-induced gene expression in recombinant human embryonic kidney cells	Baumstark-Kahn	^{13}C	75
2 Sept.	P591	22.5	Apoptosis induces by carbon ions in normal and tumor cells : determination of the relative biological efficiency using this criteria and study of the mechanisms involved	Gueulette	^{13}C	75
15 Sept.	P575	25	Radiolyse pulsée à TEL élevés avec les ions lourds. Réactivité dans les traces des radicaux libres de l'eau	Baldacchino	^{13}C	75

EXPERIMENTS CONDUCTED IN SWIFT ION PHYSICS
YEAR 2002 (continued)

Date	Exp #	Duration *hours*	Title	spokesperson	Beam	Energy *A.Mev*
12 Oct.	P628	40	Surface nano-structuring by selective sub-fs heating of clusters by swift heavy ions	Lebius	^{129}Xe	7
14 Oct.	P581	72	Etude des transformations de phases dans les oxydes	Benyaboug	^{129}Xe	7
20 Oct.		16	Tests	Betz	^{129}Xe	7
21 Oct.	P596	40	Structural modifications in LaF3 and BaF2	Trautmann	^{129}Xe	7
24 Oct.	P619	8	Hystérésis de mouillage sur des surfaces hétérogènes	Ramos	^{129}Xe	7
6 Nov.	P630	21.5	Radiolyse des macromolécules biologiques par les ions lourds de TEL . 180 keV/um. Modélisation des effets biologiques de la réaction ^{10}B(n,a) ^{7}Li.		^{36}Ar	95
	P603		High let particle-induced degradation of DNA bases			
	P593		Study of heavy ion-induced gene expression in recombinant human embryonic kidney cells			
7 Nov.	P615	12	Radiolyse pulsée de l'eau à TEL élevé. les radicaux OH*	Baldacchino	^{36}Ar	95

AVAILABLE IONS at GANIL

ION		PRODUCTION METHOD	COMPOUND	SAMPLE AVAILABLE AT GANIL
type	masse			
C	12	GAS	CO_2 - CH_3	YES
C	13	GAS	CO_2 - CH_3	YES
N	14	GAS	N_2	YES
N	15	GAS	N_2	YES
O	16	GAS	O_2	YES
O	17	GAS	O_2	YES
O	18	GAS	O_2 - CO_2	YES
F	19	GAS	SF_6	YES
Ne	20	GAS	Ne	YES
Ne	22	GAS	Ne	YES
Mg	24	OVEN	Mg	YES
Si	28	GAS	SiH_4	YES
S	32	GAS	SF_6	YES
S	36	GAS	SF_6	YES
Ar	36	GAS	Ar	YES
Ar	40	GAS	Ar	YES
Ca	40	OVEN	Ca	YES
Ca	48	OVEN	Ca - CaO	NO
Cr	50	OVEN	Cr	NO
Cr	52	OVEN	Cr	YES
Cr	54	OVEN	Cr	YES
Fe	56	MIVOC	$FeC_{10}H_{10}$	YES
Ni	58	MIVOC/OVEN	$NiC_{10}H_{10}$/NiO/Ni	YES
Ni	64	MIVOC/OVEN	$NiC_{10}H_{10}$/NiO/Ni	NO
Cu	65	OVEN	Cu	NO
Zn	64	OVEN	Zn	YES
Zn	70	OVEN	Zn	NO

AVAILABLE IONS at GANIL (continued)

ION		PRODUCTION METHOD	COMPOUND	SAMPLE AVAILABLE AT GANIL
type	masse			
Ge	74	OVEN	GeO_2	NO
Ge	76	OVEN	GeO_2	NO
Se	80	OVEN	Se	YES
Kr	78	GAS	Kr	YES
Kr	84	GAS	Kr	YES
Kr	86	GAS	Kr	YES
Nb	93	ROD/SPUTTERING	Nb	YES
Mo	92	OVEN	MoO_3	YES
Mo	96	OVEN	MoO_3	YES
Ag	107	OVEN	Ag	YES
Ag	109	OVEN	Ag	YES
Cd	106	OVEN	CdO	NO
Sn	112	OVEN	Sn/SnO	NO
Sn	116	OVEN	Sn/SnO	NO
Xe	124	GAS	Xe	NO
Te	125	OVEN	Te	NO
Xe	129	GAS	Xe	YES
Xe	132	GAS	Xe	YES
Xe	136	GAS	Xe	NO
Sm	154	ROD	Sm_2O3	NO
Gd	155	ROD	Gd_2O3	NO
Gd	157	ROD	Gd_2O3	NO
Gd	158	ROD	Gd_2O3	NO
Ta	181	ROD/SPUTTERING	Ta	YES
Pb	208	OVEN	Pb	YES
U	238	SPUTTERING	U	YES

ACCELERATED BEAMS
WITH THEIR CHARACTERISTICS

* : the intensity with the following format " > xx " corresponds to a 400 W accelerated beam with the possibility to get higher power
- the intensities correspond to a given energy. For a new energy a study must be done.
- the beams coming from SSC1 are available for the SME (Medium Energy Exit), with energies between 4 and 13 MeV/A. They can also be sent directly to all the experimental areas.

ION		CHARGE STATE	Isotopic enrichment	Max Source intensity	RF FREQUENCY	FINAL ENERGY	INTENSITY ON TARGET *
type	mass	source/final	%	µA	MHz	MeV/u	µA
C	12	4/5/6			12.13	75	>2.7
C	12	4/6	99	100	13.45	95	>2.1
C	13	2/6	99	100	8.54	35	>5.2
C	13	3/6		100	10.97	60	>3
C	13	3/6		200	12.13	75	18.5
N	14	2/7	99	200	7.938	30	>6.6
N	14	3/7		200	13.45	95	>2.1
N	15	3/7	99	200	11.35	65	>2.9
O	16	4/7/8			9.1	40	>5
O	16	3/8	99	200	9.52	44	>4.5
O	16	3/8		200	11.76	70	>2.8
O	16	4/8		200	13.45	95	>2.1
O	17	3/8	50	100	10,1	50	>3.8
O	17	4/8		100	12,75	84	>2.2
O	18	2/8	99	200	7,95	30	>5.9
O	18	3/8		200	10,1	50	>3.5
O	18	4/8		200	11,225	63	>2.8
O	18	4/8		200	12,2	76	>2.3
Ne	20	3/10	99	200	9,893	48	>4.1
Ne	20	5/10		200	13,45	95	>2.1
Ne	20	6/10		150	13,45	95	15.7
Ne	22	5/10	99	200	11	60	>3
Mg	24	5/12	79	6	11,77	70	1
Mg	24	7/12		10	13,45	95	1.5
S	36	(8)10/16	65	(60)/27	12,31	77.5	5.7
Ar	36	4/16	99	40	7,55	27.1	>5
Ar	36	6	99.5	100	8,07	4.9 (CSS1)	2.5

ION		CHARGE STATE	Isotopic enrichment	Max Source intensity	RF FREQUENCY	FINAL ENERGY	INTENSITY ON TARGET *
type	mass	source/final	%	µA	MHz	MeV/u	µA
Ar	36	5/16		60	8,19	32	>5
Ar	36	5/17		60	8,77	37	>5
Ar	36	5/17		60	9,31	42	>4
Ar	36	5/17		60	9,478	44	>4
Ar	36	10/18		160	13,45	95	15.8
Ar	40	7/18	99	100	7,94	30	>5
Ar	40	6/15		100	8,66	36	>4
Ar	40	7/17		100	9,52	43.8	>3.8
Ar	40	7/17		100	9,6	45	>3.7
Ar	40	9/17		150	11,053	60.9	>2.7
Ar	40	7/17		100	11,77	70	>2.4
Ar	40	9/18		150	12,27	76.9	>2.3
Ca	40	7/18	97	5	7,94	30	0.5
Ca	40	9/18/19			10.1	50	0.8
Ca	40	6/19		5	10,1347	50.4	0.5
Ca	40	9/20		10	13,455	95	1.3
Ca	48	8(10)/19	56	40	11	60.3	4
Cr	50	11/22	93	4	10,81	58	0.45
Cr	50	13/23		4	12,62	82	0.6
Cr	52	10/23	84	5	12,15	75	0.8
Cr	54	8			7.974	4.75 (CSS1)	0.4
Ni	58	9	100	10	7.6	4.3 (CSS1)	2
Ni	58	10/26		35	10,28	52	>3.4
Ni	58	12/26		15	11,38	65	>2.7
Ni	58	10/26		35	11,651	68.5	>2.6
Ni	58	10/26	68	35	11,95	72.5	>2.4
Ni	58	11/26		50	12,06	75	4.8
Ni	58	14/27		3	12,49	80	0.15
Ni	58	15/28	68	1	13,145	89.97	0.1
Ni	64	10/26	90	1à3	11,061	61	0.5
Ni	64	11/26		20	10.55	55	3.5
Cu	65	13/27	99	3	11,33	64.4	0.5
Zn	64	13/29	50	5	12,42	79	0.5
Zn	70	15/29	34	3	11,48	66	0.3 (enr:45%)
Ge	76	13/30	75	2	11,1	61	0.2

ION		CHARGE STATE	Isotopic enrichment	Max Source intensity	RF FREQUENCY	FINAL ENERGY	INTENSITY ON TARGET *
type	mass	source/final	%	µA	MHz	MeV/u	type
Ge	76	14/30		3.5	10.9	59.1	0.7
Kr	78	16/33	100	40	11.65	68.5	4
Kr	78	16/34	99	25	11,99	73	2
Kr	84	14/33	90	50	11	60	>2.6
Kr	84	11/31		90	9,055	39.5	>3.7
Kr	84	12/31		50	9,41	42.9	>3.4
Kr	86	12			7.765	4.5 (CSS1)	10
Kr	86	10/30	99	100	8,55	35	>3.9
Kr	86	15/34		40	11	60	2
Kr	86	16/33		45	11	58	4.4
Kr	86	12/31		55	9,43	43.1	>3.3
Mo	92	16(17)/37	98	3	10,975	60	0.2
Nb	93	13/31	100	1.3	7,28	25	0.2
Nb	93	14/33		1.3	8,075	31	0.2
Nb	93	16/36		1	10,64	56	0.2
Cd	106	21/44	80	5	11,5	66.5	0.15
Ag	107	19/40	99	4	10,28	52	0.3
Ag	107	18/38		3	8,71	36.4	0.3
Ag	109	18/38		3	8,55	35	0.1
Sn	112	22/46	99	3	11,222	63	0.2
Sn	112	17/43		3	10,8	57.9	0.2
Sn	116	16/37	96	4	7.28	25	0.2
Sn	116	16/38		4	7.95	30	0.2
Te	125	17/38	95	1	7.28	25	0.05
Te	125	17/38		1	7.55	27	0.05
Xe	124	18/44		15	9.62	45	0.27
Xe	129	15			7.1	0.273 (C0)	6
Xe	129	14/37	78	30	7.55	27	0.5
Xe	129	15/38		30	7,935	30	0.5
Xe	129	15/41		30	8,012	30.65	1.8
Xe	129	18/44		35	9,52	44	2
Xe	129	20/44		25	9,4	42.8	1.3
Xe	129	19/46		35	10,09	50	2
Xe	132	18/42	65	30	8,48	34.44	1.5
Xe	132	18/45		30	9,649	45.4	1.8

ION		CHARGE STATE	Isotopic enrichment	Max Source intensity	RF FREQUENCY	FINAL ENERGY	INTENSITY ON TARGET *
type	mass	source/final	%	µA	MHz	MeV/u	type
Xe	136	19/46		13	9,649	45.4	1.8
Sm	154	20/46	98	3	8,207	32	0.1
Gd	155	19/47	95	3.5	8,672	36.1	0.1
Gd	157	19/47		3.5	8,562	35.1	0.1
Gd	158	19/47		3.5	8,5073	34.7	0.1
Ta	181	24/55	100	8	8,66	36	0.08
Ta	181	24/57		8	9,055	40	0.08
Pb	208	25	99	5	8.2	5 (CSS1)	0.4
Pb	208	23/56	99	5	7,82	29	0.1
U	238	24/58	99	2	7,13	24	0.05

SPIRAL BEAMS: RADIOACTIVE ION BEAM INTENSITIES

The available SPIRAL radioactive beams are listed below as well as the primary beam characteristics on the ion source target (ECS) needed for the production.
The primary beam power is temporarily limited to 1.4 kW for safety reasons.
The colored figures are the experimental results. The radioactive beam intensity expected is given in the Low Energy Beamline (LEB) before acceleration in the cyclotron CIME and on the experimental target at high energy after the acceleration.

Radioactive Beam	Charge State	Intensity expected or measured (pps)		Min Energy (MeV per nucleon)	Max Energy (MeV per nucleon)	Primary Beam	Primary Beam Power on ECS Target (kW)	Primary Beam Energy (MeV per nucleon)
		LEB	Target*					
^{6}He (0.8s)	+1 +1 +1 +2	 3.8 10^{8} 2.8 10^{7}	1.7 10^{7} 3.2 10^{7} 7.6 10^{7} 5.6 10^{6}	 1.9 6.8	3.2 5 7.3 22.8	^{13}C	1.2 1.2 1.4 1.4	75
^{8}He (0.12s)	+1 +1 +1 +2 +2	 2.6 10^{5} 3.5 10^{5} 1.5 10^{5} 1.35 10^{5}	8 10^{4} 5.2 10^{4} 7 10^{4} 1.3 10^{4} 2.7 10^{4}	 4.3 4.3	3.4 3.5 4.1 15.4 16.3	^{13}C	1.2 0.9 1.4 1.4 1.4	75
^{13}N	+1 +2 +3 +4	4.7 10^{7} 8.4 10^{6} 1.4 10^{6} 1.9 10^{5}	9.3 10^{6} 1.7 10^{6} 2.8 10^{5} 3.7 10^{4}	N.F 1.7 3.7 6.5	N.F 6.5 14.5 21	^{14}N^{7+}	1.4	95
^{14}O	+1 +2 +3 +4 +5 +6	1.3 10^{7} 4 10^{6} 1.6 10^{6} 1.6 10^{6} 4.1 10^{5} 4.1 10^{5}	2.6 10^{6} 8 10^{5} 3 10^{5} 3 10^{5} 8.2 10^{4} 8.2 10^{4}	N.F 1.7 3.2 5.6 8.8 12.6	N.F 5.6 12.5 19.3 24.3 25.4	^{16}O^{8+}	1.4	95
^{15}O	+1 +2 +3 +4 +5 +6	4.3 10^{8} 1.3 10^{8} 5 10^{7} 5 10^{7} 1.3 10^{7} 1.3 10^{7}	8.6 10^{7} 2.6 10^{7} 1 10^{7} 1 10^{7} 2.6 10^{6} 2.6 10^{6}	N.F 1.7 2.8 4.9 7.7 11	N.F 4.86 10.9 17.8 22.9 25.4	^{16}O^{8+}	1.4	95
^{17}Ne (0.11s)	+5			6	19.5	^{20}Ne	1.4	95
^{18}F	+4		2 10^{5}		7.0	^{20}Ne	0.3	95
^{18}Ne (1.7s)	+2 +4 +4 +5 +7 +8 +10	5.7 10^{7} 3 10^{6} 3 10^{7} 3.2 10^{6} 5.2 10^{6} 1.2 10^{6} 6.6 10^{3}	1.1 10^{7} 1 10^{6} 6 10^{6} 6.5 10^{5} 1.1 10^{6} 2.4 10^{5} 1.3 10^{3}	1.7 3.4 5.34 10.4 13.6 21.2	3.25 7.0 12.95 18 24.8 24.8 24.8	^{20}Ne	1.4 0.3 1.4 1.4 1.4 1.4 1.4	95

Radioactive Beam	Charge State	Intensity expected or measured (pps)		Min Energy (MeV per nucleon)	Max Energy (MeV per nucleon)	Primary Beam	Primary Beam Power on ECS Target (kW)	Primary Beam Energy (MeV per nucleon)
		LEB	Target*					
^{19}Ne (17s)	+5	1.8 10^{8}	3.7 10^{7}	4.8	17	^{20}Ne	1.4	95
^{23}Ne (37s)	+(3-6)	4.2 10^{7}	8.4 10^{6}	(1.7 - 4.7)	(4.5 - 17)	^{36}S	1.4	77.5
^{24}Ne**(3.4min)	+5 +5	1.1 10^{7} 2 10^{6}	2.2 10^{6} 2 10^{5}	3	11.4	^{36}S	1.4 1.3	77.5
^{25}Ne** (0.6s)	+5	2.2 10^{6}	4.5 10^{5}	2.8	10.5	^{36}S	1.4	77.5
^{26}Ne**(0.23s)	+5	2.8 10^{5}	5.6 10^{4}	2.6	9.7	^{36}S	1.4	77.5
^{32}Ar (98ms)	+9	1.6 10^{3}	3.3 10^{2}	5.5	18.5	^{36}Ar	1.4	95
^{33}Ar (173ms)	+8	1.2 10^{5}	2.4 10^{4}	4.1	15.4	^{36}Ar	1.4	95
^{34}Ar (844ms)	+7	3.8 10^{6}	7.7 10^{5}	2.9	11.0	^{36}Ar	1.4	95
^{35}Ar (1.78s)	+8	2.1 10^{8}	4.2 10^{7}	3.6	13.7	^{36}Ar	1.4	95
^{42}Ar**(33yr)	+8	5.2 10^{7}	10^{7}	2.5	9.54	^{48}Ca$^{\$}$	0.6	60
^{43}Ar**(5.37min)	+8	3 10^{7}	6 10^{6}	2.4	9.1	^{48}Ca$^{\$}$	0.6	60
^{44}Ar**(11.87min)	+8	1.5 10^{7}	3 10^{6}	2.3	8.7	^{48}Ca$^{\$}$	0.6	60
^{45}Ar**(21.5s)	+8	7.5 10^{5}	1.5 10^{5}	2.2	8.3	^{48}Ca$^{\$}$	0.6	60
^{46}Ar**(8.4s)	+8	3 10^{5}	6 10^{4}	2.1	8	^{48}Ca$^{\$}$	0.6	60
^{72}Kr (17s)	+11 +15	2 10^{2} 3.4 10^{2}	6.8 10^{1}	3	11.4	^{78}Kr	0.4 0.8	68.5
^{73}Kr (27s)	+11 +15	3-6 10^{3} 6 10^{3}	1.2 10^{3}	2.9	11	^{78}Kr	0.4 0.8	68.5
^{74}Kr (11.5min)	+11 +15	6 10^{4} 4.3 10^{5}	10^{4} 8.6 10^{4}	2.85	2.6 10.8	^{78}Kr ^{78}Kr	0.4 0.8	68.5
^{75}Kr (4.3min)	+11 +15	5 10^{5} 2.6 10^{6}	4 10^{5}	2.8	10.5	^{78}Kr	0.4 0.8	68.5
^{76}Kr (14.8h)	+11 +11 +15	3 10^{6} 3 10^{6} 10^{7}	6 10^{5} 10^{6} 2 10^{6}	2.7	2.6 4.4 10.2	^{78}Kr ^{78}Kr ^{78}Kr	0.4 0.4 0.8	68.5
^{77}Kr (74.4min)	+11 +15	3 10^{6} 9.8 10^{8}	1.9 10^{7}	2.6	10	^{78}Kr	0.4 0.8	68.5
^{79}Kr (35h)	+15	5.9 10^{6}	1.2 10^{6}	2.5	9.5	^{78}Kr	0.8	68.5
^{81}Kr (2.3 10^{5}yr)	+15	2.5 10^{6}	5 10^{5}	2.4	9	^{78}Kr	0.8	68.5

- Available intensity for the experiment.
- ** Computed figures
- N.F = not feasible
- ^{48}Ca$^{\$}$ = ^{48}Ca is dependent on physicists.

Appendix #2

LIST OF PUBLICATIONS

ARTICLES

Les liaisons du cuivre
MONNEAU PH.
Vide 296, 2/4 (2000) 147

Mass measurements of exotic nuclei around N=Z=40 with CSS2
LALLEMAN A.S., AUGER G., MITTIG W., CHABERT M., CHARTIER M., FERME J., GILLIBERT A., LEPINE-SZILY A., LEWITOWICZ M., MOSCATELLO M.H., ORR N.A., POLITI G., SARAZIN F., SAVAJOLS H., VAN ISACKER P., VILLARI A.C.C.
GANIL – Caen, CENBG – Gradignan, CEA Saclay – Gif-sur-Yvette, IFUSP – Sao Paulo, LPC ISMRA – Caen, Catania Univ. – Catania
Hyperfine Interactions 132, 1-4 (2001) 315
Atomic Physics At Accelerators : Mass Spectrometry
Proceedings of the APAC 2000
CARGESE
19/09/2000

The mass programme at GANIL using the CSS2 and CIME cyclotrons
CHARTIER M., MITTIG W., AUGER G., CASANDJIAN J.M., CHABERT M., FERME J., FIFIELD L .K., GILLIBERT A., LALLEMAN A.S., LEPINE-SZILY A., LEWITOWICZ M., MAC CORMICK M., MOSCATELLO M.H., DE OLIVEIRA F., ORR N.A., POLITI G., SARAZIN F., SAVAJOLS H., SPITELS C., VAN ISACKER P., VILLARI A.C.C., WIESCHER M.
CENBG – Gradignan, GANIL – Caen, Australian Nat. Univ. – Canberra, CEN Saclay Gif-sur-Yvette, IFUSP – Sao Paulo, LPC ISMRA – Caen, Catania Univ. – Catania, Notre Dame Univ. – Notre Dame Hyperfine Interactions 132, 1-4 (2001) 275
Atomic Physics At Accelerators : Mass Spectrometry
Proceedings of APAC 2000
CARGESE
19/09/2000

Recent results at the Sira test bench : diffusion properties of carbon graphite and B_4C targets
LANDRE-PELLEMOINE F., ANGELIQUE J.C., BAJEAT O., BARUE C., BENNETT R., CLAPIER F., DUCOURTIEUX M., GAUBERT G., GIBOUIN S., HUGUET Y., JARDIN P., KANDRI-RODY S., LAU C., LECESNE N., LEROY R., LEWITOWICZ M., LICHTENTHALER R., MARRY C., MAUNOURY L., OBERT J., ORR N.A., PACQUET J.Y., SAINT-LAURENT M.G., STODEL C., RATAUD J.P., VILLARI A.C.C.
GANIL – Caen, LPC ISMRA – Caen, IFUSP – Sao Paulo, IPN – Orsay, CLRC RAL – Chilton
Nuclear physics A701 (2002) 491c
Fifth International Conference on Radioactive Nuclear Beams
Divonne (Fr)
27/03/00

The programme LISE : a simulation of fragment separators
TARASOV O., BAZIN D., LEWITOWICZ M., SORLIN O.
NSCL MSU – East Lansing, FLNR JINR – Dubna, GANIL – Caen, IPN – Orsay
Cyclotrons and their Applications
International Conference on Cyclotrons and their Applications.16
East Lansing (US)
13/05/01
AIP Conference Proceedings N°600 (2001) 417

Specific cyclotron correlations under space charge effects in the case of a spherical beam
BERTRAND P., RICAUD CH.
GANIL – Caen,
Cyclotrons and their Applications
International Conference on Cyclotrons and their Applications.16
East Lansing (US)
13/05/01
AIP Conference Proceedings N°600 (2001) 379

Radioactive beam diagnostics status and development at the SPIRAL facility
CHAUTARD F., BAELDE J.L., BUCAILLE F., DUNEAU P., GALARD C., LE BLAY J.P., LOYANT J.M., MARTINA L., ULRICH M., LAUNE B.
GANIL – Caen, IPN – Orsay
Cyclotrons and their Applications
International Conference on Cyclotrons and their Applications.16
East Lansing (US)
13/05/01
AIP Conference Proceedings N°600 (2001) 370

Ganil status report
MOSCATELLO M.H., BARON E., BARUE C., BERTHE C., DAVID L., DI GIACOMO M., DOLEGIEVIEZ P, JAMET C., LEHERISSIER P., LEROY R., LOYER F., PETIT E., SAVALLE A., SENECAL G.
GANIL - Caen
Cyclotrons and their Applications
International Conference on Cyclotrons and their Applications.16
East Lansing (US)
13/05/01
AIP Conference Proceedings N°600 (2001) 102

SPIRAL facility : beam dynamics and experimental tests with stable ions
VARENNE F., BERTRAND P., BIBET D., BRU B., CHAUTARD F., DUVAL M., LIEUVIN M., RICAUD CH.,
GANIL – Caen
Cyclotrons and their Applications
International Conference on Cyclotrons and their Applications.16
East Lansing (US)
13/05/01
AIP Conference Proceedings N°600 (2001) 74

Commissioning of SPIRAL, the GANIL radioactive beam facility
LIEUVIN M., BERTRAND P., BIBET D., BRU B., CHAUTARD F., DUVAL M., RICAUD CH., VARENNE F.,
GANIL – Caen
Cyclotrons and their Applications
International Conference on Cyclotrons and their Applications.16
East Lansing (US)
13/05/01
AIP Conference Proceedings N°600 (2001) 59

High intensity heavy ion beams for exotic nuclei production at GANIL
BARON E., BARUE C., BAELDE J.L., BERTHE C., BIBET D., CHAUTARD F ., JAMET C., GUDEWICZ P., LEHERISSIER P., LOYER F., MOSCATELLO M.H., PETIT E., SAVALLE A., SENENCAL G.
GANIL – Caen
Cyclotrons and their Applications
International Conference on Cyclotrons and their Applications N°16
East Lansing (US)
13/05/01
AIP Conference Proceedings N°600 (2001) 431

SYSTEMES D'IDENTIFICATION POUR SPIRAL
KANDRY-RODY S., ETASSE D., GAUTIER J.M., SAINT-LAURENT M.G., RAINE B., LEBALY J.P., LECESNE N., OLIVIER L., LAUNE B., PIQUET B., VILLARI A.C.C., WITTWER G.
IPN – Orsay, LPC ISMRA – Caen, GANIL - Caen
DE LA RADIOACTIVITE NATURELLE AUX FAISCEAUX EXOTIQUES – RECHERCHE FONDAMENTALE ET APPLICATIONS
RENCONTRE FRANCO-MAROCAINE DE PHYSIQUE NUCLÉAIRE
EL JADIDA (MA)
10/03/99

High intensity metallic ion beams from an ECR ion source at GANIL

LEHERISSIER P., BARUE C., CANET C., DUPUIS M., FLAMBARD J.L., GAUBERT G., GIBOUIN S., HUGUET Y., JAFFRES P.A., JARDIN P., LECESNE N., LEMAGNEN F., MAUNOURY L., PACQUET J.Y., PELLEMOINE-LANDRE F., RATAUD J.P.
GANIL – Caen, ISMRA – Caen
Review of Scientific Instruments 73, 2 Part.II (2002) 558

LIMBE: a new facility for low energy beams

MAUNOURY L., LEROY R., BEEN T., GAUBERT G., GUILLAUME L., LECLERC D., LEPOUTRE A., MOUTON V., PACQUET J.Y., RAMILLON J.M., VICQUELIN R. AND THE GANIL ION PRODUCTION GROUP
CIRIL – Caen, GANIL – Caen
Review of Scientific Instruments 73, 2 Part.II (2002) 561

Ions source development at GANIL for radioactive beams and high state ions

LEROY R., BARUE C., CANET C., DUPUIS M., FLAMBARD J.L., GAUBERT G., GIBOUIN S., HUGUET Y., JARDIN P., LECESNE N., LEHERISSIER P., LEMAGNEN F., MAUNOURY L., PACQUET J.Y., PELLEMOINE-LANDRE F., RATAUD J.P., SAINT-LAURENT M.G., VILLARI A.C.C.
GANIL – Caen, CIRIL – Caen
Review of Scientific Instruments 73, 2 Part.II (2002) 711

Mono 1000 : A simple and efficient 2,45 GHz electron cyclotron resonance ions source using a new magnetic structure concept

JARDIN P., BARUE C., CANET C., DUPUIS M., FLAMBARD J.L., GAUBERT G., LECESNE N., LEHERISSIER P., LEMAGNEN F., LEROY R., PACQUET J.Y., PELLEMOINE-LANDRE F., RATAUD J.P., SAINT-LAURENT M.G., VILLARI A.C.C.
GANIL – Caen
Review of Scientific Instruments 73, 2 Part.II (2002) 789

Minimono : An ultra compact permanent magnet ion source for singly charged ions

GAUBERT G., BARUE C., CANET C., CORNELL J., DUPUIS M., FARABOLINI W., FLAMBARD J.L., GOREL P., JARDIN P., LECESNE N., LEHERISSIER P., LEMAGNEN F., LEROY R., PACQUET J.Y., SAINT-LAURENT M.G., VILLARI A.C.C.
Review of Scientific Instruments 74, 2 (2003) 956

PREPRINTS

GANIL A 00 01
Cryogenic system for a thin solid hydrogen target
Dolégiéviez P., Robillard Ph., Gallardo Ph., Ozille M., Heuzé D.
GANIL – Caen

GANIL S 00 01
Dynamique de faisceau dans CIME en Harmonique 3
Chautard F., Bourgarel M.P.
GANIL – Caen

GANIL S 00 02
Etalonnage des tensions HF de CIME par la méthode des rayons X
Di Giacomo M., Villari A.C.C., Leyge J.F., Menager L., Allal D., Bouvet G., Lechartier M., Schmiechen G.
GANIL – Caen

GANIL A 01 01
GANIL Status report
Moscatello M.H., Baron E., Barué C., Berthe C., David L., Di Giacomo M., Dolégiéviez P, jamet C., Lehérissier P., Leroy R., Loyer F., Petit E., Savalle A., Sénécal G.
GANIL - Caen

GANIL A 01 02
High intensity heavy ion beams for exotic nuclei production at GANIL
Baron E., Bru C., Baelde J.L., Berthe C., Bibet D., Chautard F., Jamet C., Gudewicz P., Leherissier P., Loyer F., Moscatello M-H., Petit E., Savalle A., Sénécal G.
GANIL - Caen

GANIL A 01 03
Radiaoctive beam diagnostics status and development at the SPIRAL facility
Chautard F., Baelde J.L., Bucaille F., Duneau P., Galard C., Le Blay J.P., Loyant J.M., Martina L., Ulrich M., Launé B.
GANIL – Caen, IPN - Orsay

GANIL A 01 04
SPIRAL facility : beam dynamics and experiemntal tests with stable ions
Varenne F., Bertrand P., Bibet D., Bru B., Chautard F., Duval M., Lieuvin M., Ricaud Ch.,
GANIL - Caen

GANIL A 01 05
LIMBE: a new facility for low energy beams
Maunoury L., Leroy R., Been T., Gaubert G., Guillaume L., Leclerc D., Lepoutre A., Mouton V., Pacquet J.Y., Ramillon J.M., Vicquelin R. and the GANIL ion production group
CIRIL – Caen, GANIL - Caen

GANIL A 01 06
High intensity metallic ion beams from an ECR ion source at GANIL
Lehérissier P., Barué C., Canet C., Dupuis M., Flambard J.L., Gaubert G., Gibouin S., Huguet Y., Jaffres P.A., Jardin P., Lecesne N., Lemagnen F., Maunoury L., Pacquet J.Y., Pellemoine-Landré F., Rataud J.P.
GANIL – Caen, ISMRA - Caen

GANIL A 01 07
Ions source development at GANIL for radioactive beams and high state ions
Leroy R., Barué C., Canet C., Dupuis M., Flambard J.L., Gaubert G., Gibouin S., Huguet Y., Jardin P., Lecesne N., Lehérissier P., Lemagnen F., Maunoury L., Pacquet J.Y., Pellemoine-Landré F., Rataud J.P., Saint-Laurent M.G., Villari A.C.C.
GANIL – Caen, CIRIL – Caen

GANIL S 01 01
The accelerated ISOL technique and the SPIRAL project
Villari A.C.C. and the Spiral Group
GANIL – Caen

GANIL S 01 02
Temperature simulations for the SPIRAL ISOL target
Maunoury L., Bajeat O., Lichtenthäller R., Villari A.C.C.
GANIL – Caen, CIRIL – Caen, IPN – Orsay, IFUSP – Sao Paulo

GANIL S 01 03
Production and post acceleration scheme for SPIRAL
Bibet D. and the SPIRAL group
GANIL – Caen

GANIL A 02 01

Mono 1000 : a simple and efficient 2.45 GHz ECRIS using a new magnetic structure concept
Jardin P., Barué C., Canet C., Dupuis M., Flambard J.L., Gaubert G., Lecesne N., Lehérissier P., Lemagnen F., Leroy R., Pacquet J.Y., Pellemoine F., Rataud J.P.,
Saint-Laurent M.G., Villari A.C.C.
GANIL – Caen

GANIL A 02 02
Metallic ion beam developments

Barué C., Canet C., Dupuis M., Flambard J.L., Gaubert G., Huguet Y., Jardin P., Lecesne N., Lehérissier P., Lemagnen F., Leroy R., Pacquet J.Y., Pellemoine-Landré F.,
GANIL – Caen

GANIL A 02 03
The LIMBE facility and the ARIBE project
Maunoury L., Been T., Huber B.A., Lebius H., Leclerc D., Lepoutre A., Mouton V., Ramillon, J.M., Vicquelin R., Leroy R., Pacquet J.Y.

CIRIL – Caen, GANIL - Caen

GANIL A 02 04

MINIMONO : an ultra-compact permanent magnet ions source for singly charged ions
Gaubert G., Barué C., Canet C., Cornell J., Dupuis M., Farabolini W., Flambard J.L., Gorel P., Jardin P., Lecesne N., Leherissier P., Lemagnen F., Leroy R., Pacquet J.Y., Saint-Laurent M.G., Villari A.C.C.
GANIL – Caen

GANIL A 02 05

Evaluation of a LINUX based control system for GANIL
David L
GANIL – Caen

REPORTS

GANIL R 00 01
A low enetrgy facility at SPIRAL-GANIL
Auger G., Bocage F., Jacquot B.
GANIL – Caen

GANIL R 00 02
Réalisation d'un banc de tests de sources d'ions
Gaubert G.
GANIL – Caen

GANIL R 00 03
TWIST II Workshop on Target and Ion Source Technology
Villari A.C.C., Saint-Laurent M.G.
GANIL – Caen

GANIL R 00 04
Positionnement géométrique du spectromètre LISE (Ligne d'Ions Super Epluchés) installé au GANIL, associé à un ensemble détecteur modulaire de neutrons
Beunard R.

GANIL R 01 01
Opération et développement 1999
Baron E.
GANIL – Caen

GANIL R 01 02
High intensity beams at GANIL and future opportunities: LINAG
Auger G., Mittig W., Moscatello M.H., Villari A.C.C.
GANIL – Caen

GANIL R 01 03
SPIRAL Phase-II
Saint Laurent M.G., Lhersonneau G. Aystö J., Brandenburg S., Mueller A.C., Vervier J.,
GANIL – Caen, Jyväskylä Univ. – Jyväskylä, KVI – Groningen, IPN – Orsay, centre de recherches du Cyclotron – Louvain-la-Neuve

GANIL R 01 04
SPIRAL II : preliminary design study

GANIL R 02 02

Caractérisation de l'intensité d'un faisceau d'ions lourds par mesure de sa composante électromagnétique haute fréquence
Mariette C.
GANIL – Caen

GANIL R 02 03

SPIRAL II Project (electron option)
Loyer F., Saha H., Savalle A., Royet P., Loyer F.
GANIL – Caen

GANIL R 02 04
Conceptual design report : Individual radioactive ion injection, cooling and storage in a ring

Meshkov I., Mittig W., Roussel-Chomaz P., Sidorin A., Smirnov A., Syresin E.,
GANIL – Caen, JINR - Dubna

GANIL R 02 05
Projet IRRSUD Rapport de fin de projet
Loyer F.
GANIL – Caen

GANIL R 02 06
Rapport de spectrométrie visible avec la source ECR MONO 1001
Tuske O., Maunoury L., Pacquet J.Y.
GANIL – Caen, CIRIL – Caen

GANIL R 02 07
MONO 1001
Pacquet J.Y., Leroy R., Barué C., Canet C., Dubois M., Dupuis M., Flambard J.L., Gaubert G., Jardin P., Kantas S., Lecesne N., Leherissier P., Lemagnen F., Maunoury L., Pellemoine F., Saint-Laurent M.G., Tuske O., Villari A.C.C.
GANIL- Caen, PANTECHNIK – Caen, CIRIL - Caen